STUDY AND DESIGN OF A MICRO PULSED PLASMA THRUSTER FOR A 3U CUBESAT

Xavier Almenar Cerdán

São Carlos School of Engineering

University of São Paulo

A thesis submitted for the degree of

Aerospace Engineering

2016 June

Abstract

Cubesats are the doors leading to space research for universities, enterprises and even governments. With the increase in use of these nanosatellites, propulsion systems for them must be developed so that they become useful in a wide range of missions. Micro pulsed plasma thrusters might be the solution key. In this project PPTs will be studied, possible ways for optimisation and a new design will be proposed.

Contents

List of Figures iii

List of Tables v

1 Introduction 1

2 Electric propulsion 3

2.1 Electro-thermal 3

2.2 Electro-magnetic 4

2.3 Electro-dynamic 5

3 Pulse Plasma Thruster Fundamentals 7

3.1 Discharge description 8

3.1.1 Initiation 9

3.1.2 Propagation 10

3.1.3 Expulsion 10

4 Classification of Pulsed Plasma Thrusters 13

4.1 By Electrode Geometry 13

4.1.1 Parallel Plate Electrodes 14

4.1.2 Coaxial Electrodes 15

4.1.3 Linear or Z-Pinch 16

4.1.4 Inverse Z-Pinch 19

4.2 By Propellant 21

4.2.1 Solid or Ablated PPT's 21

4.2.2 Gaseous propellant PPT's 24

4.2.3 Liquid propellant PPT's 25

5 Mathematical Modelling **27**

5.1 One Dimensional Circuit Equation 27

5.2 Thrust Transfer Equation 29

5.3 Plasma Resistance Equation 30

5.4 Late Time Ablation Additional Resistance 33

6 Optimisation of a PPT **35**

7 PPT Design **43**

7.1 Mission requirements 43

7.2 Type of PPT 45

7.3 Electrical circuit 47

7.4 Design 49

8 Extra activities **55**

8.1 Zenith 56

8.1.1 Parachute development 56

8.1.1.1 Choice of type of parachute 57

8.1.1.2 Sizing, calculations and parameters 59

8.1.2 Results 60

8.2 INPE e ITA 61

8.2.1 INPE, São José dos Campos 61

8.2.2 ITA 63

8.2.3 LCP, INPE, Cachoeira Paulista 63

9 Conclusion and Future Work **65**

References **67**

List of Figures

3.1 Typical PPT schema 8
3.2 Deformed current sheet at the exit of a gas-fed pulsed plasma thruster [15] 11

4.1 Parallel Plates PPT [42] 14
4.2 Divergent Plates PPT [40] 14
4.3 Coaxial PPT: linear outer electrode [13] 15
4.4 Coaxial PPT: divergent outer electrode [42] 15
4.5 Z-Pinch PPT [13] 17
4.6 Section of a Z-Pinch PPT [31] 17
4.7 Section of Z-Pinch PPT showing central orifice [31] 18
4.8 Section of a Z-Pinch PPT with central orifice and spike [31] 18
4.9 Comparison between working principles 20
4.10 Inverse-Pinch PPT: electrode design 20
4.11 Breech-fed Ablative PPTs 22

5.1 Electrical schema of a typical PPT 28
5.2 Electron Temperature and density profile predicted in the SSC model [28] 32
5.3 Electron number density data for the NASA High Thrust PPT [26] . . . 32
5.4 Plasma resistance compared with the current waveform [28] 33

6.1 Inductance and Resistance over different positions for different flare angle electrode [29] 36
6.2 Ablation rates over flare angle [29] 37
6.3 Calculated results of plasma velocity distribution (14 degree) [29] 37
6.4 Impulse bit, specific implse and efficiency over flare angle [29] 38
6.5 Efficiency over Aspect ratio varying surface [28] 39

6.6 Changing mass bit for the LES 8/9 thruster [28] 40
6.7 Changing mass bit at various aspect ratios for the LES 8/9 PPT [28] . . 40

7.1 Semi-empirical specific impulse trend with E/A [11] 45
7.2 Input voltage, discharge circuit and electrical PPT schema 48
7.3 Input and output voltage values reaching the PPT 49
7.4 Frontal view of the proposed PPT 50
7.5 Top view of the proposed PPT using amplification 51
7.6 Required specific impulsed with respect to the propellant mass 52
7.7 PPT inserted in a 3U CubeSat 53

8.1 Schema of a Cross-Type Parachute 59
8.2 Photo taken at the Garatéa gondola in the stratosphere, with bacteria being exposed (All Credits to Zenith) 61
8.3 Engineering models of a NanosatC-Br1 and NanosatC-Br2 62
8.4 Zenith student group at LIT laboratory of INPE 62
8.5 Perspective projection of the modules distribution in the 6U structure (Credits: ITA) 63
8.6 Pulsed Plasma Thruster developed at INPE [8] 64

List of Tables

4.1 PPT Characteristics 23

5.1 Initial results for the LES 8/9 PPT from the SSC model [28] 33
5.2 The equivalent late time ablation resistances added to the model [28] . . 34
5.3 Initial results for the LES 8/9 PPT from the SSC model [28] 34

8.1 Drag Coefficients depending on the type of parachute 58

LIST OF TABLES

1

Introduction

Outer space has been fascinating humanity from our existence. However, the interesting aspect is not the doubt of knowing what is out there but to help us learn about our planet. Since 1957, thousands of satellites have been launched and orbited the Earth. Nowadays, with the advances in miniaturization and capability increase of electronic technology, smaller satellites are on the rise. Microsatellites, nanosatellites, picosatellites and even femtosatellites are being used due to the reduced cost of deployment and the option to launch in multiples.

CubeSats are a type of nanosatellite for space research made up of 10x10x10 cm cubes that have become the most proper ones for academic institutions to explore this field. These nanosats have flown with no propulsion in space while they were used for university experiments but governments and industry are increasing their interest in them. Orbit changing, formation flying or attitude control are some of the essential actions CubeSats must be able to perform so that a wider range of missions becomes available.

Micro propulsion is the key to make these nanosats capable of reaching more targets. Cold gas thrusters, chemical, electric propulsion or even solar sails are being studied to be used in CubeSats. Electric propulsion uses electric energy to accelerate propellant to high speed and there are many different types such as Hall-effect thrusters, ion thrusters, pulsed plasma thrusters, electrospray thrusters and resistojets.

2

Electric propulsion

Chemical devices normally heat a gas to create thrust but electric ones can produce thrust by several different methods. There are three main types of electric devices: electro-thermal (such as Resisjojets and Arcjets), which use electricity to heat a gaseous propellant; electro-magnetic (such as Ion and Hall Effect thrusters); electro-dynamic devices that ionize and accelerate a propellant electrodynamically and magnetodynamic thrusters from which the most common are the Pulsed Plasma Thruster.

2.1 Electro-thermal

Arcjets and resistojets have been used succesfully in flight for station keeping. They have very high specific impulses (around 1000s), which makes them extremely efficient in the sense that theres no need of storing a large amount of propellant for long duration missions. Anyway, they arent so small taking into account theyre electric devices (about a few kilograms and between 10 and 20cm in length) so they are used often for mini-satellites and micro-satellites but not smaller ones.

Arcjets use an arc between a cathode and an anode (one located before a constrictor and the other one in the nozzle) The created arc goes through the constrictor heating a gas, which is then expanded through the nozzle.

Electro-thermal devices are electrical devices although they dont differ much from chemical propulsion systems because they heat a gas that expands through the nozzle to produce thrust due to the increase of pressure. No electromagnetic fields are used to ionize or accelerate the gas, which makes them different from the other electrical propulsion systems.

2.2 Electro-magnetic

To this category belong the well-known Ion and Hall Effect thrusters. Ion thrusters have already been used in important deep space missions, as the DEEP-SPACE-1. Their sizes can vary depending on the requirements needed as they can be small with a few Watts of power until several thousand-watt sizes. Gaseous propellant is used so they need of a fuel tank to operate but since their specific impulse is also very high (1500-3000s), small tanks are valid even for long missions. Thats why they are used in many satellites, from micro to big ones).

Ion thrusters ionize gas instead of heating it. Gas is injected into the chamber where goes through an electric field, introducing the neutral atoms to high-energy free electrons, what produces a collision that ionizes the neutral gas. At the opening there are grids that contain the electrons, being one of the grids held at high potential and the other one to the ground, making a potential difference, which repels the electrons but attracts the ions, accelerating them to the opening of the grids. This acceleration is what creates thrust. Then other electrons are emitted from another cathode so that the ions do not leave the thruster.

Hall Effect thrusters ionize the gas in a different way. An electromagnet is surrounding the chamber creating a radial magnetic field inside it, which attracts some free electrodes emitted from a external cathode. These electrons are captured by the magnetic field and their charge makes them spin along the magnetic field lines, producing what is know as Hall Effect. Then a neutral propellant gas is introduced into the chamber and passes through those electrons forming ions. Theses ions are accelerated out of the chamber by the electric and magnetic fields because of the Lorentz Force. The electrons that had been emitted by the cathode but were not attracted by the magnetic fields, are combined with the ions forming a quasi neutral plasma. Thrust is therefore created by the momentum exchange.

2.3 Electro-dynamic

Pulsed plasma thrusters are the most common example of electro-dynamic propulsion devices. While the previous devices seen before use a gas as a propellant, PPTs typically use a solid one (normally Teflon). This propellant is kept inside the thruster so theres no need of a tank to storage it as in other propulsion systems. The thrust produced with PPTs is also smaller (from milli- to micro-Newtons) and they are ideal for nano- and pico-satellites due to their small size (few centimeters or less). Afterwards, a deeper insight of PPTs and micro-PPTs will be made.

Another interesting device with respect to the electro-dynamic propulsion are the electrodynamic tethers (EDTs) which consist of long conducting wires that can operate as generators converting kinetic to electrical energy or as propeller converting electrical to kinetic energy. They have many applications for spacecrafts, being a low-budget option which uses the Earth magnetic field and and the current flow in the tether element to create an electromagnetic force when orbiting the planet.

3

Pulse Plasma Thruster Fundamentals

A pulsed plasma thruster is an electromagnetic propulsion system that ablates, ionizes normally a solid propellant and generates thrust by accelerating the plasma through the Lorentz Force with the induced magnetic field.

The PPTs typical design has got a pair of electrodes charged by capacitors to an electrical potential difference ranging from hundreds to few kilovolts. The same way, the stored energy level can vary from few Joules to many hundreds and therefore its power consumption might value less than a Watts or hundreds depending on the pulse repetition rate.

Normally a spark plug initiates the discharge due to the reduced dielectric strength of the space between the pair of electrodes. In solid propellant PPTs the discharge is originated across surface of the insulator (usually Teflon), which is ablated and ionized from the surface. There are other PPTs that use a gas or a liquid as propellant, where the discharge also ionizes their particles forming a plasma sheet that is accelerated by the Lorentz Force. This electromagnetic force is created by the current flow through the plasma sheet and the self-induced magnetic field generated by the discharge current itself.

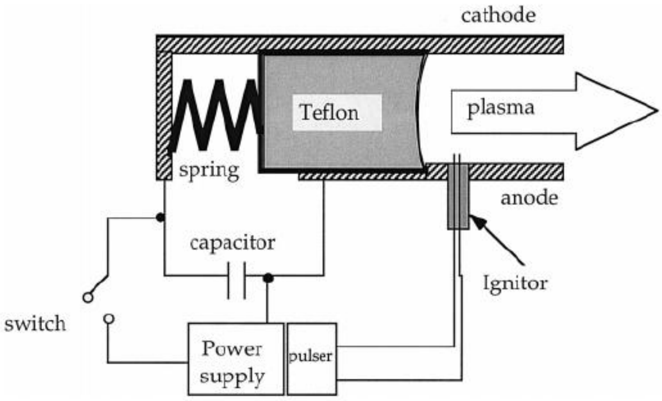

Figure 3.1: Typical PPT schema

$$\vec{F} = q\vec{v} \times \vec{B}$$

This Lorentz force is directed to the end of the electrodes so that the plasma sheet is accelerated towards the exit of the thruster. But this plasma is not only accelerated by the electromagnetic force but also due to gasdynamic thrust because it is created a pressure field around the thruster surfaces due to the heat produced by the discharge. These two effects coexist and it is thought gasdynamic thrust has more importance when there is a bigger quantity of propellant in the thruster discharge chamber [4, 5, 36, 41].

When the capacitor is already drained or the plasma sheet has left the inner space between the electrodes, the discharge finishes. With the thrust its produced a specific impulse on the range of 10 microNs 1mNs and a poor efficiency normally between 5%-20%. [3]

3.1 Discharge description

In this section it will be discussed the development of the plasma sheet along with the dynamics of the discharge produced, dividing it in three different stages: initiation, propagation and expulsion [12, 13, 42].

3.1.1 Initiation

First, what mainly needs the current discharge to take place are high voltages (between 10^2 V and 10^5 V) and high currents too (around 10^4 A) so that the thruster is able to get a better performance. Its needed then a device that can store a big amount of electrical energy and supply it in a fast way. Thats why capacitors are a good choice, because they have the ability to store a sensible amount of electrical energy, considering the low voltage input the satellite would provide.

There are also gas-fed pulsed plasma thrusters, where the inner space between electrodes is filled with the gaseous propellant. The discharge can be produced when more and more propellant is added, increasing the gas density and since that reduces the dielectric strength, at some point triggers the capacitor discharge. However, since that way the timing of the discharge is not controlled, it is normally used a spark plug to initiate it.

In solid propellant PPTs spark plugs are nearly always necessary so that the discharge takes place. A trigger electrode charged to very high voltages (1-50kV) produces a first discharge ionizing a small amount of propellant. The plasma created by that first discharge lowers the dielectric strength between the electrodes and the breakdown comes, releasing the energy from the capacitor.

Trigger electrodes are very important for the discharge because depending on their position and their quantity, the stability and uniformity of the discharge will vary.

After the breakdown, a low intensity glow discharge is diffused along the whole electrodes and immediately only focuses in a thin arc, the plasma sheet, at the beginning of the thruster where the inductance is the lowest. This is called skin effect. The plasma created by the discharge maintains the arc between the electrodes. Also, the energy released in the discharge gets the propellant to very high temperatures causing its partial ionization.

With respect to the quantity of propellant, it may not seem important but depending on how much there is available, the discharge is affected. If there is less propellant than the optimal, the stability of the arc and the thrust process can be affected. The other way, having extra propellant could affect mainly the specific impulse and the thruster efficiency.

Moreover, the discharge must occupy the whole thruster section, have a good conductivity to minimise resistive losses and a current density that maximise the current sheet impermeability. The factors that have an influence on this are the discharge circuit parameters (to determine a high current peak), the chamber geometry (optimising the current distribution along the section) and the propellant density (enough mass to sustain the arc but not too much to avoid overloading it).

3.1.2 Propagation

The arc has already been formed, as previously said, where the inductance is minimum, the closer to the capacitor as possible. From that point it is important the Lorentz force, which is created by the interaction between the self-inducted magnetic field and the discharge current. Under the influence of this force, the arc is accelerated to the end of the electrodes until leaving the thruster. The magnetic field created is such that is perpendicular to the section and the Lorentz force always pointing towards the right sense.

It has to be considered too that in order to maximise the quantity of propellant being accelerated, distortions and porosities are not good characteristics into the structure of the arc.

3.1.3 Expulsion

This part of the process is crucial. When the plasma sheet arrived to the end of the electrodes is expelled towards the exterior. What is ideal is that this plasma sheet has a uniform velocity profile, parallel to the electrodes so that the losses are minimized.

Moreover, it is extremely important to synchronize the discharge with the sheet position so that it ends at the same moment as the plasma leaves the chamber. The problem is that when by reaching the end of the electrodes there is still some

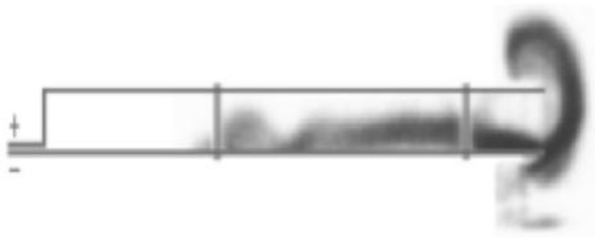

Figure 3.2: Deformed current sheet at the exit of a gas-fed pulsed plasma thruster [15]

energy in the capacitors, the discharge is not finished. Since there is current flowing through the plasma, it will try to keep connected to the electrodes, making a curve shape in the plasma sheet that leads to important losses.

That happens because at the same time that the plasma sheet tries to remain plugged to the electrodes, the Lorentz force is also pushing it towards the exterior, producing the curve seen in the picture, from where it can be deducted the loss of velocity vectors in the right direction to create thrust.

Sometimes, flared electrodes or even nozzles are used sometimes to recover some of the thermal energy that has been deposited into the plasma.

Finally, it is possible that a new discharge is produced before the sheet reaches the end when the discharge current is oscillatory. The secondary discharge appears before the current being reversed, remaining stationary where the inductance is minimized, short-circuiting the previous current sheet and preventing it from being accelerated. That is why most of the energy that goes into that process is considered as wasted.

4

Classification of Pulsed Plasma Thrusters

Apart from the nature of the propellant, PPTs have also normally be divided into different groups depending on their geometry and the way the propellant is stored.

4.1 By Electrode Geometry

Differentiating pulsed plasma thrusters by the electrode geometry leads us to four main groups:

- Parallel Plate Electrodes PPTs
- Coaxial Electrodes
- Linear or Z-Pinch
- Inverse Z-Pinch

4.1.1 Parallel Plate Electrodes

As previously seen in the picture of a PPT, the typical configuration is a two parallel rectangular electrode plates. It is the simplest one but not the optimal so other configurations are used, such as ending up with flared electrodes and more recently, tongue shaped ones.

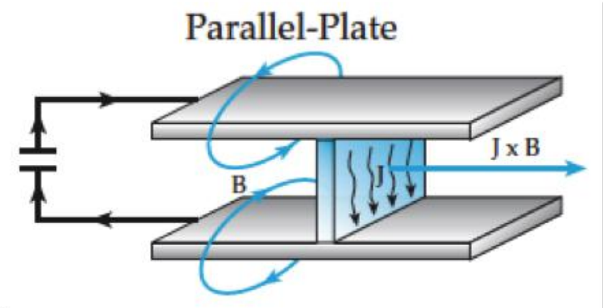

Figure 4.1: Parallel Plates PPT [42]

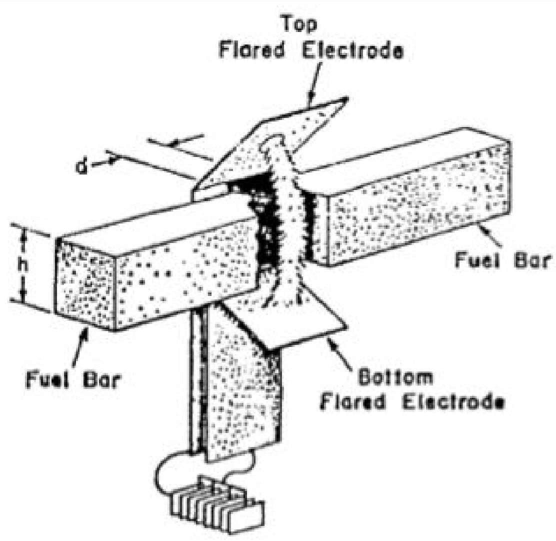

Figure 4.2: Divergent Plates PPT [40]

In this type of PPTs, the relevant geometrical parameters are the length of the electrodes and their aspect ratio h/w (h is the height or distance from one electrode to the other and w is the width of the electrodes) with determine the inductance of the circuit. The main advantage of this geometry is its simplicity to be made but it leads to some disadvantages because of that too: the rectangular electrodes means having edges that will affect the self-induced magnetic field, bad influencing the thrust.

4.1.2 Coaxial Electrodes

Radial symmetry geometries are the best ones to model analytically and numerically so the coaxial electrode configuration has been applied to PPTs too. The external electrode can be either straight forming a cylinder or with a divergence angle, approaching to the flared plate electrode configuration

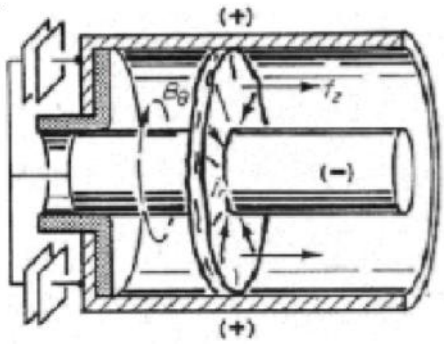

Figure 4.3: Coaxial PPT: linear outer electrode [13]

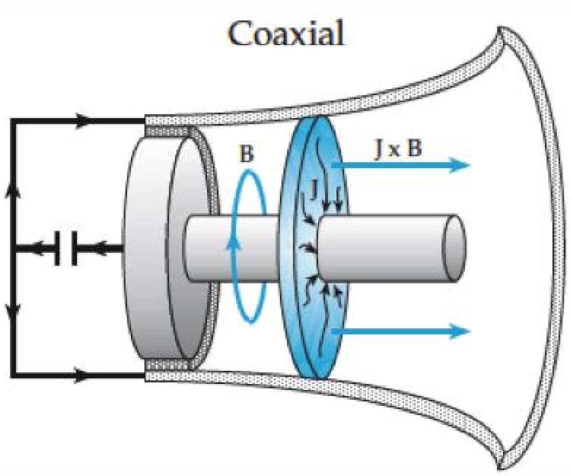

Figure 4.4: Coaxial PPT: divergent outer electrode [42]

After the discharge is triggered, it is assumed the structure of an annular sheet. The self-inducted magnetic field has a toroidal shape around the central electrode and the interaction between current and the magnetic field creates the electromagnetic force pushing the current sheet towards the exit of the thruster.

Since radial electrodes maintain symmetry and no edges, in the case of the rectangular electrodes, there are no field distortions. However, the problem with this configuration is related with the discharge current density because it is not uniform in the whole radius but it varies with $1/r$. Close to the external electrode the electromagnetic force is proportional to $1/r^2$. It is supposed that this might be the cause of the effects appearing with this type of PPTs: plume divergence, radial current instability and sheet canting when there is a loss of orthogonality between the electrodes and the current arc) [13]

The trigger device is relevant with this geometry because the initiation process should be as uniform as possible so that the plasma accelerations does not suffer more distortions. One solution is to equippe it with it multiple triggers acting with the same timing [30].

4.1.3 Linear or Z-Pinch

The design of this type of PPT is also simple: two disc-shaped electrodes separated by insulating walls linked to a energy-storing device as the capacitor. When the propellant is gaseous, the gas can be introduced in the space between the electrodes. When solid propellant is used, the walls themselves can act as propellant if made of Teflon, for instance.

Due to the skin effect previously seen, when the discharge is triggered, a thin cylindrical layer of current is being formed near the insulating surface because it is where the circuit impedance gets to the minimum.

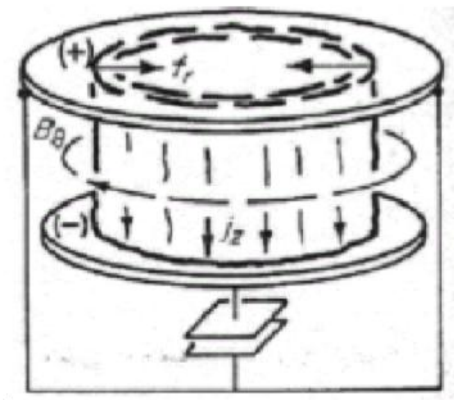

Figure 4.5: Z-Pinch PPT [13]

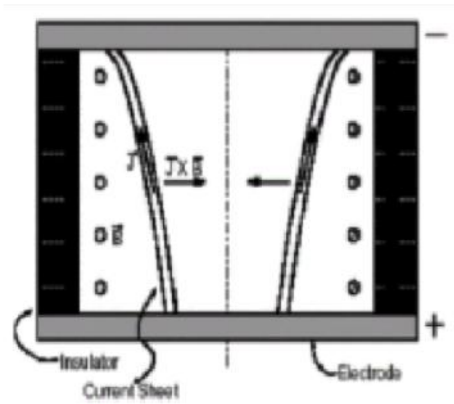

Figure 4.6: Section of a Z-Pinch PPT [31]

As in the previous configuration, a toroidal magnetic field is created, with its whole flux inside the chamber. However, in this case, the Lorentz force created by the iteration between current and self-induced magnetic field accelerates the arc radially, taking the plasma to the centre of the thruster. At first, this configuration device was used to create high-density high-temperature plasma for nuclear fusion purposes. When taken to the propulsion field, it was introduced an orifice in one of the electrodes so that the propellant finds a strong axial pressure gradient and produce thrust in that axial direction [1, 31].

Afterwards, it was tried to use nozzles at the orifice but even taking into account the advantages due to the plasma thermal recovery, it seemed it did not compensate the losses associated of adding the nozzles.

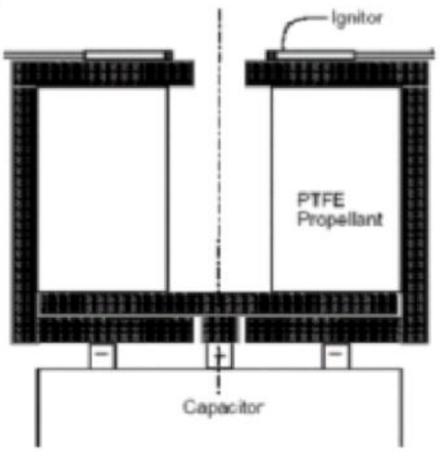

Figure 4.7: Section of Z-Pinch PPT showing central orifice [31]

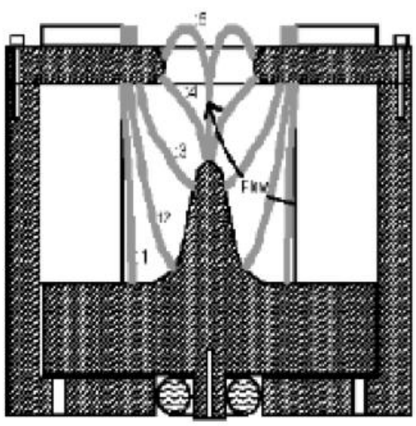

Figure 4.8: Section of a Z-Pinch PPT with central orifice and spike [31]

With this toroidal configuration the main trouble is to convert from radial to axial motion. That is why some considerations have to be taken into account when making the choice of the electrodes and in which one the orifice should be made. In some studies it has been observed that the arc moves more rapidly to the anode than the cathode during the discharge propagation [15, 23, 32]. This produces an inclination of the accelerated plasma layer that can be used to convert the direction of the advancement. This is called zipper effect because of the discharge shape. That is why this type of thruster configuration is called Z-Pinch. As it is seen in one image, the configuration was modified with an anode having a spike protruding towards the hole in the cathode. Since the discharge travels faster along the anode, this protrusion influences the flux rotation in a better way, being the plasma now more focused at the centre of the thruster, enhancing the axial thrust.

Linear-Pinch PPTs are attractive then due to their geometry because it provides uniform current density and magnetic field on the whole plasma surface. Moreover, when using gaseous propellant, they have a good dynamic efficiency: the discharge starts at the maximum radium point of the chamber so the major propellant is accelerated when the arc is still at low velocities.

Since they are easy to design and manufacture and is capable of adapting when getting smaller, it is very useful for microsatellites.

Furthermore, there is another advantage is that the plasma plume focuses more thank in other configurations because of the hole through which the plasma is expelled.

Finally, the radial direction assumed by the ablated propellant (when using solid ones) limits the chance of vaporised macro-particles to be expelled out of the thruster after the discharge has extinguished: only a part of these particles leaves the thruster and the remaining ones stay, and can be accelerated in the following discharge. That is why with this configuration there is a very good propellant utilisation.

4.1.4 Inverse Z-Pinch

Inverse Pinch PPTs also use the radial configuration but are a bit different from the Linear Pinch ones because here the capacitor and the line that closes the circuit are closer to the axis than the arc (not like in the other case where the arc is the closest to the thruster axis. Again, it is found a toroidal magnetical field but this time with the opposite direction. The Lorentz force is produced too due to the mixture between the current and the magnetic field but it moves the arc away from the axis. The current sheet is then accelerated the other way around comparing to the Linear Pinch thrusters.

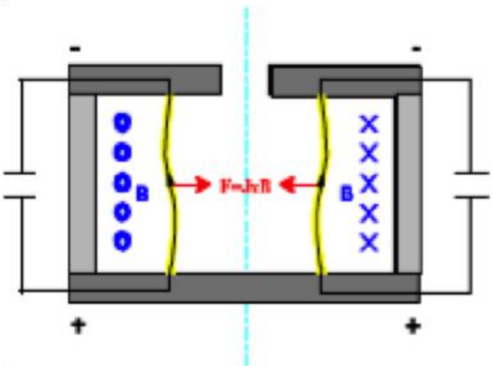

(a) Z-Pinch PPT working principle

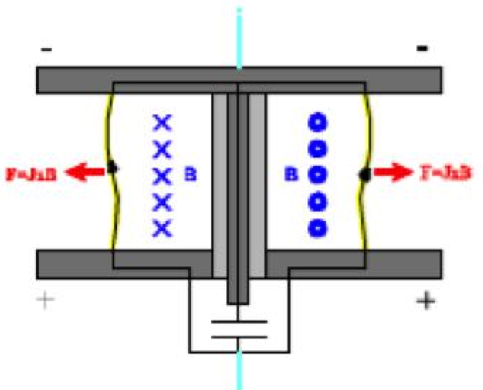

(b) Inverse-Pinch PPT working principle

Figure 4.9: Comparison between working principles

A good aspect about this configuration is that it is possible to change the shape of the electrodes so that a maximal axial acceleration can be obtained. Indeed, curving the anode and shorting the cathode leads to the formation of an 90 degree arc path.

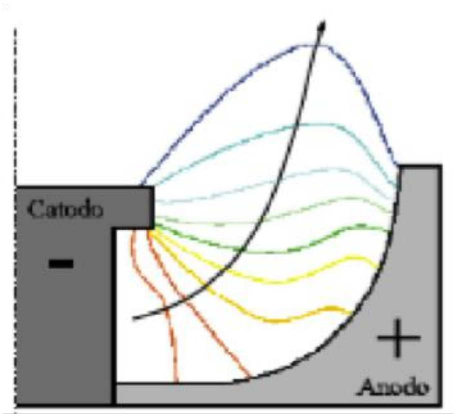

Figure 4.10: Inverse-Pinch PPT: electrode design

Moreover, the reciprocal position of the electrodes has the influence of the arc behaviour, canting to advance more rapidly in the anode. This configuration is of course available to be used with solid propellants because they have a symmetric distribution of the current density in the discharge, which is good for the ablation of the propellant.

Finally, these PPTs have very low operational temperatures, being able to maintain it below 673 K that is the decomposition temperature of Teflon so the evaporation of particles (that bad influences the performance of the thrusters) is reduced.

4.2 By Propellant

The other common way to differentiate between pulsed plasma thrusters is the type of propellant used or, more specifically, the phase state in which it is used. That way it is found PPTs that use solid propellants, gas or liquid ones.

4.2.1 Solid or Ablated PPT's

Solid propellant PPTs have been extensively used for a long time in the flight field because they have some aspects that made them more suitable for some space applications such as:

- Absence of pipework or tanks, making it easier to integrate on a spacecraft
- Propellant is stable and easy to storage
- There are no moving parts
- During periods of inactivity there is no risk of propellant leakage
- Simple designs that improve reliability

These solid propellant PPTs are called ablative PPTs because the discharge produced between the electrodes ablates the surface (or surfaces) of the propellant, forming the plasma sheet where the current will flow maintaining the discharge, being accelerated by the electromagnetic force.

A-PPTs are able to provide a reliable low-intensity thrust perfect for precise manoeuvring [35] and they have high specific impulses (between 300s and 2000s) [3]

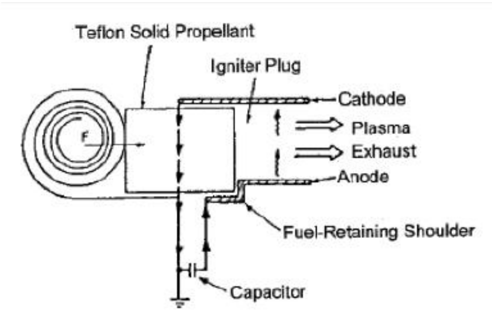

(a) Parallel-plate electrodes [3]

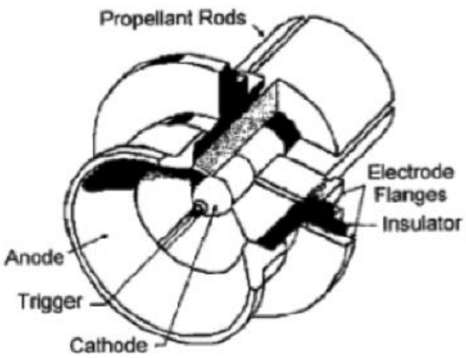

(b) Coaxial-plate electrodes [3]

Figure 4.11: Breech-fed Ablative PPTs

with a mean power range of 1-300W [10]. For instance, there are some thrusters that require only a few Watts of power and have been successfully tested and flown [**? ? ?**]

Ablative PPTs can also be divided into two different groups depending on the position and the geometry of the propellant rod: some present a single propellant rod at the thruster breech being known as breech-fed PPTs and the others are names side-fed PPTs because two or more propellant bars go into the inner space between the electrodes, arriving close to where the discharge initially focuses.

Where the propellant bars are located not only is a matter of geometry but of performance too: in breech-fed PPTs the propellant can only be ablated at the beginning of the discharge when the current sheet is close to the breech while in side-fed thrusters the discharge can keep ablating the propellant bars after some time too while the plasma being accelerated because the bars might be part of the thruster walls.

In solid propellant thruster it is interesting to be aware that in many studies it has been shown that the discharge energy is directly proportional to the impulse bit. Not only but also that depending if it uses breech-fed or side-fed system, fixed values for this appear [3, 10, 14, 38]:

$$\left(\frac{I_{bit}}{E_0}\right)_{breech-feed} = 16\mu Ns/J \tag{4.1}$$

$$\left(\frac{I_{bit}}{E_0}\right)_{side-feed} = 23\mu Ns/J \tag{4.2}$$

Previously, it was mentioned that gasdynamic played its role in accelerating the plasma sheet but it was not specified how much. There are some studies that have shown that for this type of thruster, the gasdynamic contribution can be up to 25%-50%, which is a considerably part of the total thrust then. Impulse bit is related to the discharge energy, and so does the mass bit, whose ratio to the stored energy takes values in the range of $1 - 10\mu g/J$.

In this table the main characteristics of the ablative PPTs are shown:

Solid Propellant PPTs	
Propellant	Teflon
Stored Energy Range (J)	1 - 100
Impulse Bit range (μNs)	10 - 1000
Impulse bit over stored energy ($\mu Ns/J$)	$\sim 16(breech - fed) \sim 23(side - fed)$
Mass bit over stored energy ratio $\mu g/J$)	1-10
Specific impulse range (s)	300 - 2000
Efficiency (%)	1 - 20

Table 4.1: PPT Characteristics

The main problem of these thrusters then is the low efficiency, which happens normally for low energy thrusters but in more recent ones efficiencies are higher [2, 27].

The low efficiency is probably caused by the poor utilisation of the propellant because only a part of the ablated propellant is well accelerated [21]. Furthermore, the surface of the propellant keeps suffering ablation after the discharge and stay like that up to $300\mu s$ [6]. This effect is the well-known called Late Time Ablation. Part of the energy is completely wasted due to the ablation of propellant that will not be accelerated electromagnetically and slowly leaves the thruster, not contributing to thrust but to decrease the specific impulse. However, there is a technique some have developed to fight that phenomena, which is to accelerate this late-ablated propellant with a secondary discharge but still the results are not as good as desired [19, 20] .

The material used as propellant is normally Teflon because it has been proved to be the most suitable for this application although its decomposition temperature (673 K) does not help the prevention of late time ablation effect, which clearly affects negatively the performances and causes spacecraft contamination. Other materials have been tested such as polyethylene, acrylic plastics and other thermoplastics [3] but they have not proved to lead to a better performance. Nevertheless, Teflon impregnated with carbon did made some improvements in the performances [25], not like porous Teflon.

4.2.2 Gaseous propellant PPT's

The first PPTs to be ever tested were using gaseous propellant. Like ablative pulsed plasma thrusters, they have high specific impulse, they are small, precise and with low power consumption. However, they have some advantages with respect to the solid propellant PPTs [17]:

- Absence of any contamination issue
- Improved throttling capabilities due to the independence of the mass bit on the discharge current
- Wider range of achievable specific impulses
- Improved repeatability because there are no shot to shot variations derived from the propellant ablation irregularities)
- Absence of large particles that negatively affect the performances
- Low production rate of slow neutrals
- The low dielectric strength of the gas allows operation at reduced voltages (100 400V compared to 1.2kV in A-PPTs)

Working at lower voltages makes the propulsion system easier due to the possibility of using lower impedances so there is a better maching in the discharge circuit between the capacitor and the current sheet. Moreover, lower voltages will reduce the safety regulations for humans when dealing with the device.

Furthermore, efficiency ranges normally get higher than the ones of solid propellant thrusters [17, 41].

However, as mentioned before, tanks and plumbing are needed to store the propellant. The gas used is normally Xenon, Argon or water vapour [43]. Also, it is necessary a fast operating valve to limit the waste of propellant between two consecutive shots. Apart from reducing the simplicity and the ease of integration, these components also affect the system reliability. Since in the past these components were not as advanced as now (especially the fast-valves) the gas-propellant thrusters were much less reliable than solid propellant ones.

Nowadays then, they came back into consideration and advancements are being made with the improvements in the valves and development of the pulse forming networks, allowing the appearance of multiple thruster discharges while the valve is still open, which minimise the loss of propellant. However, these solutions are not adequate in size for micro thrusters.

4.2.3 Liquid propellant PPT's

Nowadays, apart from the improvement in the new advancements of gas-propellant thrusters, liquid propellant PPTs have been developed [57]. Both of them have some similarities: they have many advantages solid propellants have but also tanks, plumbing and valves. Nevertheless, water is the usual used propellant, which stored in liquid state allows equipment to be much less restrictive and slower valves can be used due to the lower diffusion rate of a liquid when compared to a gas.

However, there are some concerns on reliability and these thrusters have not been developed much. Fortunately, in the late years some studies have been performed testing liquid propellant PPTs which show improvement and competitive results compared to ablative PPTs[14, 39]

5

Mathematical Modelling

The work done by Laperriere [7] has been used afterwards by other studies due to the building of a mathematical model to simulate and optimise pulsed plasma thrusters. The work starts by replicating his parallel plate electromechanical model based on a set of coupled differential equations. Nevertheless, the model was not perfect and the Surrey Space Center expanded it and optimised it so that accuracy was increased [28]. Specifics include integrating the impulse bit rather than using a trapezoidal summation, it includes the effects of simple gas dynamic forces and includes a variable resistance model based on current carrying plasmas. The one dimensional parallel plate slug mass model can be considered in three parts, the one dimensional circuit equation, the thrust transfer equation and the plasma resistance model.

5.1 One Dimensional Circuit Equation

Considering the following electrical circuit composed of a capacitor, two electrodes and the wires that connect them:

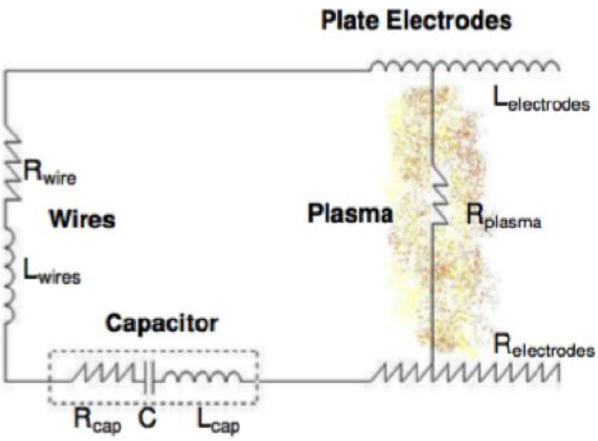

Figure 5.1: Electrical schema of a typical PPT

To find the self-inducted magnetic field $\vec{B}$ it is referred back to the assumption of the ideal one turn solenoid, where assuming a uniform current sheet K i.e. uniform current per unit width passes through electrodes and wires with infinite conductivity creating a conducting circuit, with the electrodes width being much greater than the height. Assuming infinite conductivity is valid in our theory for the wires and electrodes but in plasma there is a finite conductivity that leads to the current sheet K having a thickness δ. Taking into account the boundary conditions and instigating the Gauss continuity condition the magnetic field can be calculated. In the normal direction:

$$\nabla.\mu_0\overline{H} = 0 \tag{5.1}$$

$$\oint_s \mu_0\overline{H}.dA = 0 \tag{5.2}$$

$$\overline{n}.\frac{B_{inc}}{\mu_0} = 0 \tag{5.3}$$

In the tangential direction:

$$\nabla \times \overline{H} = \overline{j} \tag{5.4}$$

$$\oint_s \overline{H}.ds = \int \overline{j}dA \tag{5.5}$$

$$\overline{n} \times \frac{B_{inc}}{\mu_0} = K \tag{5.6}$$

$$B_{inc} = \mu_0 K\hat{y} = \mu_0 \frac{I(t)}{w}\hat{y} \tag{5.7}$$

The one dimensional circuit equation is then:

$$\begin{aligned} V_0 - \frac{1}{C}\int_0^t I(t)dt = I(t)\Big[R_{cap} + R_{wires} + R_{electrodes} + R_{plasma}\Big] + \frac{dx_s}{dt}\mu_0\frac{h}{w}I(t) \\ + \frac{dI(t)}{dt}\left(L_{cap} + L_{wires} + \mu_0\frac{h}{w}x_s(t) + \mu_0\frac{h}{w}\frac{\delta}{2}\right) \end{aligned} \tag{5.8}$$

5.2 Thrust Transfer Equation

As explained previously, the force on the plasma sheet in PPTs is produced due to the effect of the gas dynamics and the magnetic acceleration from the Lorentz force. Then:

$$\frac{d}{dt}\left[m(t)\frac{dx(t)}{dt}\right] = \sum F_T(t) = F_{initial} + F_{gas} + F_{em} \tag{5.9}$$

Assuming neutral charge the force equivalent equation becomes:

$$\frac{d}{dt}\frac{dx(t)}{dt} + m(t)\frac{dx^2(t)}{d^2t} = \frac{d}{dt}mU_0 + h \cdot w \cdot n_0 \cdot k_B \cdot T_e(t) + \int_V (j \times B)dV \tag{5.10}$$

And solving it for the electromagnetic force inside the current sheet:

$$\int_V (j \times B)dV = \int_{x_s}^{x_s+\delta}\int_0^w\int_0^h \mu_0\frac{I(t)}{w}\left[1 - \frac{x - x_s}{\delta}\right]\hat{y}.\left(-\frac{I(t)}{w\delta}\right)\hat{z}dzdydx \tag{5.11}$$

$$\int_V (j \times B) dV = \frac{1}{2}\mu_0 \frac{h}{w}[I(t)]^2 \hat{x} \tag{5.12}$$

This model assumes that when the plasma is formed, there is no additional mass accumulated to the plasma while it is accelerated down the discharge chamber $dm(t)/dt = 0, m(t) = m_0$. Then the force equation becomes:

$$m_0 \frac{dx^2(t)}{d^2t} = \frac{d}{dt} m_0 U_0 + h \cdot w \cdot n_0 \cdot k_B \cdot T_e(t) + \frac{1}{2}\mu_0 \frac{h}{w}[I(t)]^2 \tag{5.13}$$

To expand Laperrieres work, the thrust transfer equation is expanded to include the effects of initial momentum and gas pressure in the discharge chamber. Initially there is no need of expanding it for considering the initial momentum for a pair of electrodes but considering it, evaluation of the two-stage pulsed plasma thruster will be possible more accurately because the plasma will have a momentum when entering the second pair of electrodes. Therefore, in order to analyse the effects of large density plasma plumes on the general thrust, gas dynamic force is included, too.

5.3 Plasma Resistance Equation

An equation for the power plasma holds within the discharge chamber working from first principles using Maxwells equations in the MHD approximation [37]:

$$I(t)V_{plasma} = \int_V \frac{j^2}{\sigma_{plasma}} dV + \int_V U \cdot (j \times B) dV + \int_V j \frac{\partial A}{\partial t} dV \tag{5.14}$$

where the first term on the right side is the Joule heating that can be expressed as:

$$\int_V \frac{j^2}{\sigma_{plasma}} dV = \int_{x_s}^{x_s+\delta} \int_0^w \int_0^h \frac{[I(t)]^2}{w^2 \delta^2 \sigma_{plasma}} dz dy dx = \frac{h \cdot [I(t)]^2}{w \delta \sigma_{plasma}} \tag{5.15}$$

Assuming that all the resistance is due to the joule heating term, the effects of the power due to the Lorentz force and inductive term are neglected in this model. The resistance of the plasma due to ohmic heating is then [38]:

$$R_{plasma} = \frac{e_i e \sqrt{m_e} ln\wedge}{6\pi\sqrt{3}\varepsilon_0^2 (k_B T_e(t))^{3/2}} \tag{5.16}$$

where the symbol lander is the plasma parameter and represents the typical number of particles in the Debye sphere [9]:

$$\wedge = 4\pi n_e \lambda_D^3 \tag{5.17}$$

Assuming that for every ion there is a free electron, being then a quasi-neutral plasma, Saha approximation can be applied to predict the number of electrons in the plasma:

$$n_0 = \frac{1}{h^3}(2\pi m_e k_B T_e(t))^{3/2} e^{\left(\frac{-I_e}{k_B T_e(t)}\right)} \tag{5.18}$$

with the Ionisation energy of a Teflon molecule being 8.445eV [24]. Taking the assumption that the electron temperature is much greater than the ion temperature and considering the system as a one-turn solenoid $B = \mu I(t)$ we can derive the electron temperature from the diamagnetic current [38]:

$$I_{diamagnetic} = I(t) = (k_B T_e(t)) \frac{B \times \nabla n_0}{B^2} \tag{5.19}$$

The most relevant particle drift is the diamagnetic drift velocity. The profile of the electron temperature and density was calculated by SSC and comparing the model results and the experimental ones, it can be seen that the model is only valid until 20.000 K, when the electron number decrease experimentally. This is probably by the Saha approximation because at that temperature double ionization occurs. Since nominal electron temperatures can range from 40.000 K to 120.000 K, the resistance model is not accurate. To solve that, there should be done a resistance model with plasma number density equation with the distribution of ions.

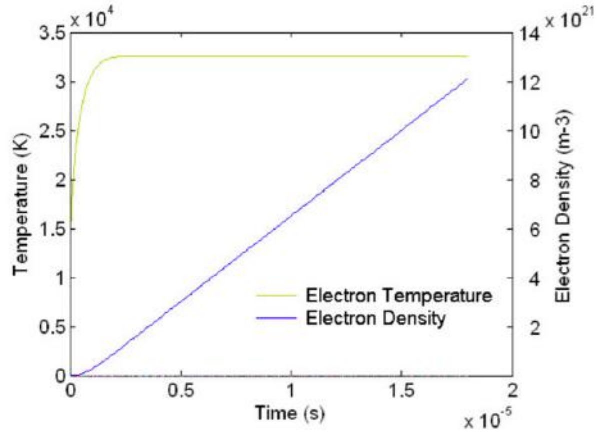

Figure 5.2: Electron Temperature and density profile predicted in the SSC model [28]

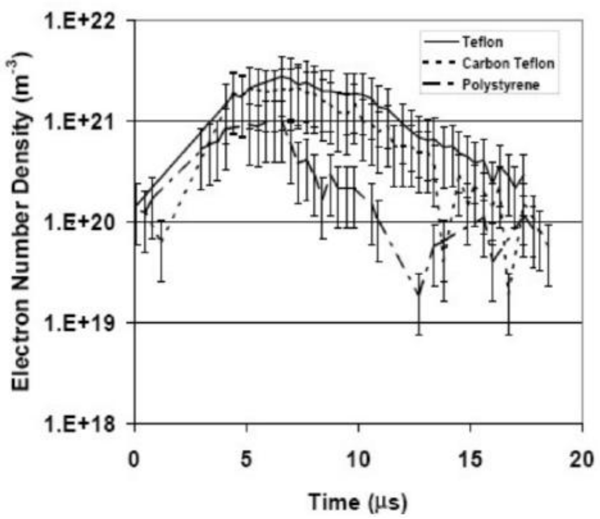

Figure 5.3: Electron number density data for the NASA High Thrust PPT [26]

Comparing the modelled plasma resistance with the current waveform, it is shown that the plasma resistance remains practically constant but when the current is reversed, a pike appears in the plasma resistance.

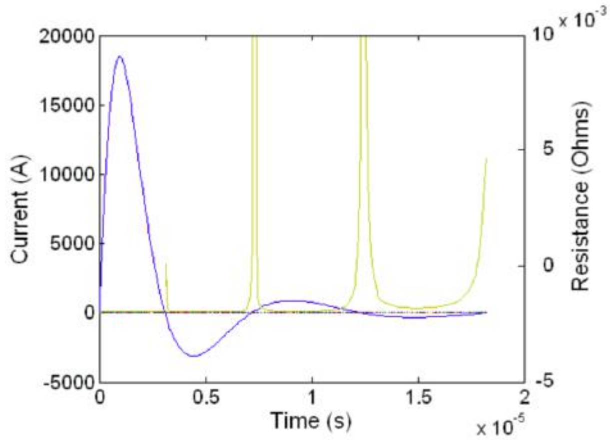

Figure 5.4: Plasma resistance compared with the current waveform [28]

5.4 Late Time Ablation Additional Resistance

When running the model, it appears there are considerable differences between the experimental and simulated results in Laperrieres work [7], but it might fall within the acceptable uncertainty of the plasma resistance, as Waltz investigated [26]:

	Specific impulse (s)		Impulse bit ($\mu N.s$)		Thruster efficiency (%)	
LES 8/9	Exp.	Sim.	Exp.	Sim.	Exp.	Sim.
	1000	1200	297	335	6.0	9.8

Table 5.1: Initial results for the LES 8/9 PPT from the SSC model [28]

The solution for this might be the one addressed by SSC adding a resistance value for the Late Time Ablation effect.

$$R_{total} = R_{plasma} + R_{electrodes} + R_{cap} + R_{wires} + R_{LTA} \tag{5.20}$$

This resistance value is found from the experimental results so that they match with the simulated ones. For instance, it has been tested with 3 different PPTs and the values have been:

PPT	R_{LTA}
LES 6	0.08
LES 8/9	0.01
Dawgstar	0.15

Table 5.2: The equivalent late time ablation resistances added to the model [28]

	Specific impulse (s)		Impulse bit ($\mu N.s$)		Thruster efficiency (%)	
	Exp.	Sim.	Exp.	Sim.	Exp.	Sim.
LES 6	312	312	32	31	3.0	2.5
LES 8/9	1000	998	297	278	6.0	6.8
Dawgstar	266	271	66	67	1.8	1.8

Table 5.3: Initial results for the LES 8/9 PPT from the SSC model [28]

Like that, when re-evaluating the experimental results, this time the difference between experimental and simulated results are very low relatively:

6

Optimisation of a PPT

In this chapter it will be studied how pulsed plasma thruster can have a better performance taking into account the available parameters. Parallel plate PPTs maximise on electromagnetic acceleration. There are many methods to increase the accelerating force: by increasing the magnetic field or by increasing the current density. Laperriere and Kimura, among others, have studied increasing the magnetic field but it was found that although there were increases in impulse bits around 50% [7, 16], the mass of the PPT would increase too much for space flight due to external magnets.

Therefore, maximising the current density is what seems that should be done. Decreasing the chamber width so that the width of the plasma sheets also decreases, makes the current density constricted but with the same amount of current going through it. Since this constriction would increase the current density, so would increase the electromagnetic acceleration.

Moreover, using flared electrodes leads to an increase in the plasma effective resistance, more initial stored electrical energy is into discharge energy and more propellant is ablated. However, fraction of the ablated propellant is being accelerated electromagnetically and the propellant utility decreases [29].

The Chinese study made about the influence of the electrode flare angle shows there would be an optimal flare angle so that performance of the PPT is maximised.

It is interesting to check some parameters depending on the configuration.

For instance, changing this flare angle in the PPT to see how inductance and resistances vary. The developed experiment was made for angles of 0 degree, 14 degree, 27 degree and 37 degree:

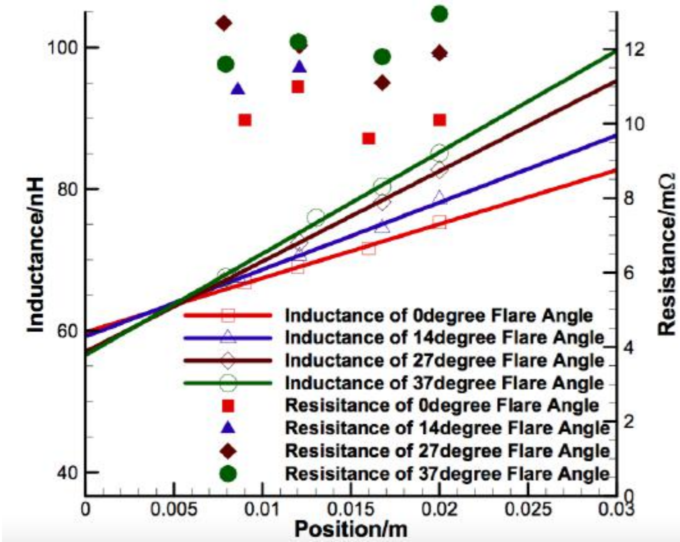

Figure 6.1: Inductance and Resistance over different positions for different flare angle electrode [29]

Increasing the flare angle results in an increase in the equivalent inductance Leq, resistance Req, effective plasma resistance Rp, and the energy transfer efficiency tr, whereas peak current Imax exhibits a decreasing trend. The increase in energy transfer efficiency means more initial stored electrical energy is converted into discharge energy, which may be caused by the increase of effective plasma resistance.

With respect to the ablated mass, increasing the flare angle leads to an increase in the ablated mass of propellant per pulse, too.

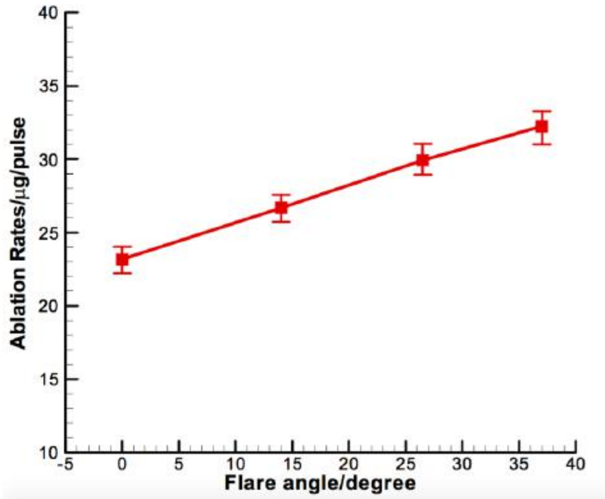

Figure 6.2: Ablation rates over flare angle [29]

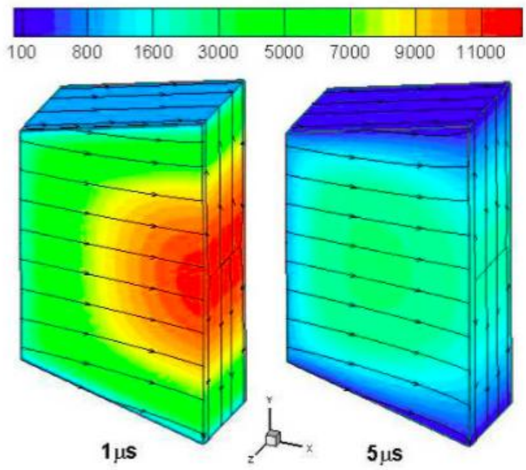

Figure 6.3: Calculated results of plasma velocity distribution (14 degree) [29]

It seems that portion of the kinetic energy is consumed because of the plasma moving along the expansion direction, leading to a decrease in the plasma ejecting velocity in the propellant ablation surface. An increase in the ablated mass might be good but always taking into account the available energy so that it is possible ablate that additional part of Teflon.

Other relevant aspects are the specific impulse, the impulse bit and the efficiency. Checking all of this in the following graph, it is shown that the maximum performance is obtained for a flare angle of 27 degree and then the thruster performance decreases. Although it has only been evaluated for 4 different angles, it gives an approximate idea of what occurs.

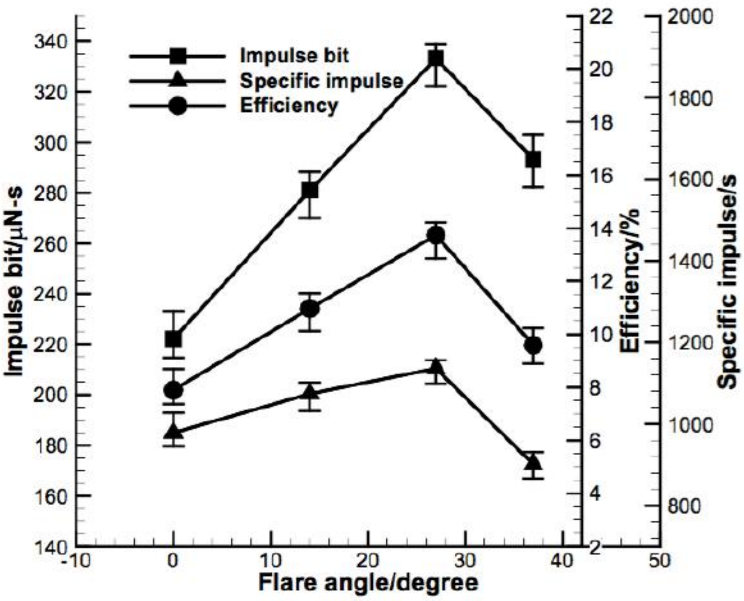

Figure 6.4: Impulse bit, specific implse and efficiency over flare angle [29]

Because of decreasing of the discharge current, even with the inductance gradient increase with the flare angle, the electromagnetic acceleration occupy 76% of the total impulse bit at 26 degree while 81% at 0 degree [29]. Moreover, increasing the flare angle leads to an increase in the ablated propellant mass. However, at the same time when increasing the flare angle, the fraction of mass being electromagnetically accelerated decreases. Another aspect it should be considered is the propellant surface to check if thruster efficiency depends on it. SSC made a simulation varying the surface and the Aspect Ratio (remembering that the Aspect Ratio (AR) is the height between the electrodes divided by the width of the space (h/w)), showing there is no crucial trust efficiency difference between the different configurations.

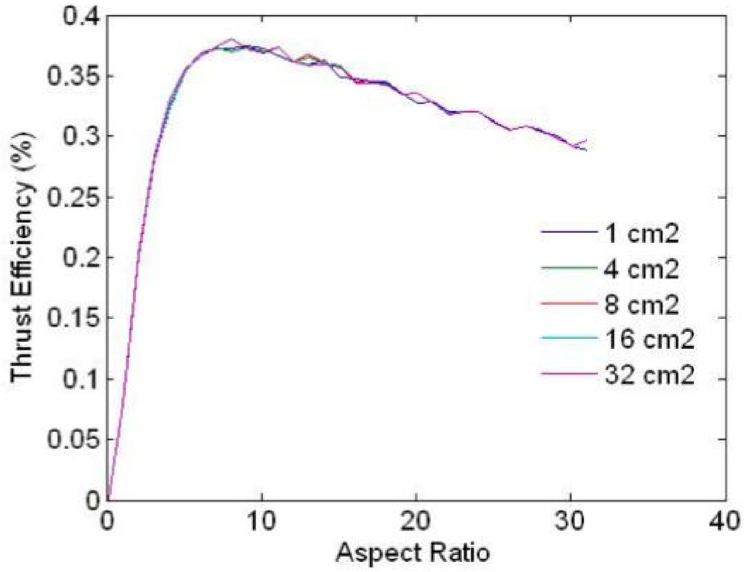

Figure 6.5: Efficiency over Aspect ratio varying surface [28]

However, it must be remembered that an increase in the propellant surface to be ablated, it needs a minimal energy available or the ablation will not occur as desired. That is why the critical device is the capacitor because depending on it the maximum available energy will be established.

The mass bit, which is the amount of propellant ablated per discharge, is difficult to manipulate without using alternative gas or liquid fuels with complex feed mechanisms [1]. In solid fuels PPTs the mass bit has got shot to shot variations. Testing for the LES 8/9 PPT capacitor it is shown that there is an ideal ablated mass, which in this case would be $10\mu g$.

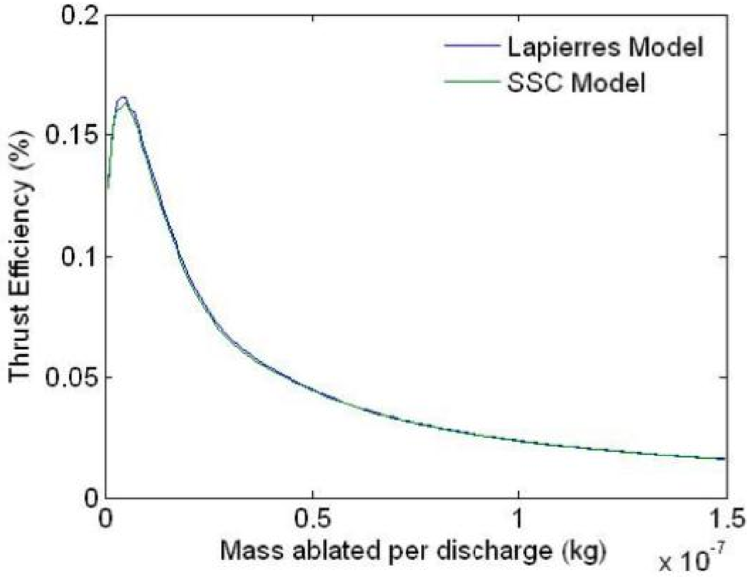

Figure 6.6: Changing mass bit for the LES 8/9 thruster [28]

In addition, the aspect ratio is a parameter to consider. Checking the difference in thrust for the LES 8/9 PPT, the aspect radio should be considered as one of the most important aspects to consider when building this kind of thrusters:

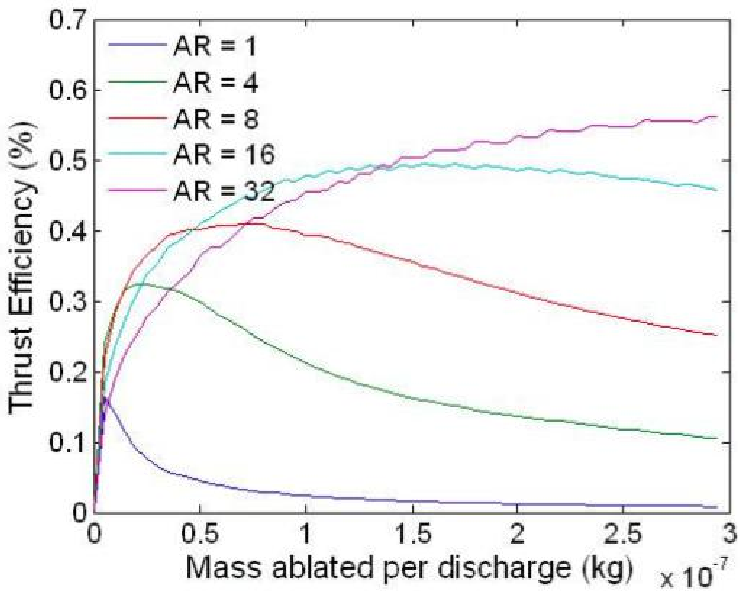

Figure 6.7: Changing mass bit at various aspect ratios for the LES 8/9 PPT [28]

It is seen that when aspect ratio is increased, the mass bit required to reach an optimal performance increases. Moreover, with higher aspect ratios, the increase in mass but has much less effect on the performance. Specifically, we can see that if that thruster had been made with an aspect ratio of 4 instead of 1 and increasing a bit the propellant surface so that the ablated mass increases a bit, the thruster performance would have doubled.

With respect to the shape of the electrodes, it has been seen the effect of the flare electrode angle but there is also another aspect that might optimise a pulsed plasma thruster. Improving the parameter L' leads to a maximization the electromagnetic part of the impulse bit. Ending the electrode with a tongue shape has been tested by many Europeans in the recent years and has been proved to increase that L' parameter, being then beneficial for the thruster. [17, 23, 32, 33, 34, 35].

Furthermore, it has been found that the electromagnetic acceleration is directly proportional to the ratio between the inductance variation during the discharge and the initial discharge circuit inductance

Investigating other electrical parameters it can be seen that it is important to keep inductance to a minimum. Therefore, from the equation of the electrical circuit we can deduct inductance can be reduced by:

- optimizing the aspect ratio
- decreasing the current sheet thickness
- decreasing the discharge length
- decreasing the rate of current change in the discharge pulse
- reducing the inductance of the capacitor and electrical wires

Finally, it is important to remark the importance of the electrode dimensions because if the electrodes are too short the propellant is expelled when there is still energy stored in the capacitors, whereas, if the electrodes are too long, the friction with the walls would slow down the propellant, reducing the specific impulse [23].

7

PPT Design

In this chapter the thruster design will be presented, together with a justification of the solutions that have been adopted. Some of the choices made during the design process were immediate and forced by the nature of the application and the associated strict volume and mass requirements: for example, right from the start it was decided to use a solid propellant, in order to avoid all the problems coming from the tanks required by liquid or gas-fed thrusters (tank volume, pipework, fast operating valves, etc.). Furthermore, taking into account its heritage from other thrusters and bearing in mind the issues discussed in section 4.2, pure Teflon was selected as propellant material.

7.1 Mission requirements

One purpose of this study is to design a micro PPT that controls a 3U CubeSat. The thruster could be mounted on a standard PCB card, normally adopted by the CubeSat Kit bus. Because of that, the maximum dimensions where the thruster and the electronics must fit are 90x90x25 mm (already considering the card thickness).

With respect to the mass, each CubeSat unit of 10x10x10cm as a mass of no more than 1.33kg and commonly is adopted a maximum of 1kg. Taking into account that in the unit where the thruster will be placed there will be other devices for experiments or power related items, a limit of 150g can be established. With respect to the power consumption, due to the limited availability of it in these nano satellites because of the constrained dimensions of solar panels, a maximum limit of 0.3W of average power consumption should be applied.

A total impulse should be established so that the pulsed plasma thruster reaches a minimum level of thrust depending on the mission. In this example it is wanted the PPT to be used as a control attitude device. Impulse bit requirements for attitude control have been estimated previously by Blandino [22]. Based on impulsive manoeuvres, and a dead band time between firings of 20 and 100 seconds, respectively, required impulse bits for a 1 kg may be as low as $29\mu Ns$ for 1 degree (17 mrad) pointing requirements for 100 seconds dead band intervals, and decrease for smaller pointing requirements of 0.02 mrad to as little as $0.034\mu Ns$.

Taking into account the impulse bit requirements mentioned above, for a long period mission it could be established 30 Ns as the total impulse the thruster should be capable of providing.

One of the main parameters found to affect the thruster performances in terms of propellant consumption and specific impulse is the ratio of the shot energy to the propellant area exposed to the discharge E/A: the higher the energy per area ratio the higher the values of the specific impulse [3, 10]. In particular it was found that the specific impulse varies less than linearly with E/A [3, 10] and relations have been established by Guman and Pulambo (with different configurations of the same thruster) and Gessini and Paccani (with different thrusters):

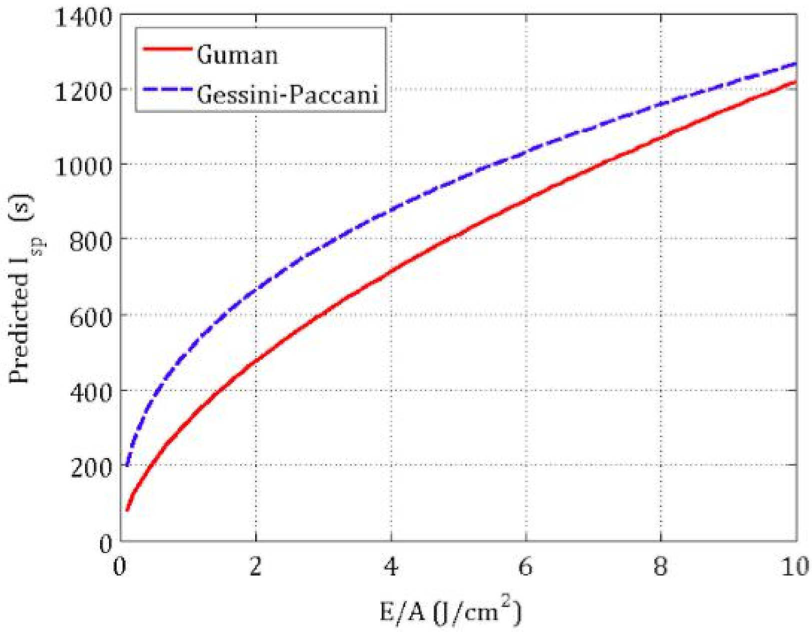

Figure 7.1: Semi-empirical specific impulse trend with E/A [11]

Very high values of the energy to propellant surface ratio lead to an excessive increase in the Teflon surface, which is negative because increases Late Time Ablation effects. However, for smaller values of E/A, as a result of poor Teflon ablation and decomposition, a film of carbon is usually deposited on the propellant surfaces, on the thruster backplate and on the sidewalls. This thin conductive layer is more difficult to evaporate in comparison to Teflon, and therefore, if the carbon film is developed it cannot be evaporated under the typical PPT conditions: as the film grows, it could eventually short the electrodes causing a complete system failure. Researches have shown that with this ratio being a bit more of 1.5 - 2 problems are minimised [40].

7.2 Type of PPT

With respect to the electrodes, only simple geometries were taken into account, with the Z-Pinch and inverse pinch configurations being discarded due to the difficulty to scale down to the dimensions required by Cubesat applications. Coaxial geometries were excluded instead because Teflon-fed coaxial PPTs are usually characterised by a propellant acceleration mechanism that is essentially thermodynamic and, therefore, they provide a lower specific impulse that could potentially not meet the mission requirements. Therefore, a linear plate electrode configuration was selected for the thruster, whose design is described in details in section 7.4.

As seen in the optimisation chapter, one of the crucial aspects was the aspect ratio ($AR = h/w$) being h the distance between the electrodes and w the electrodes width. Higher values of AR lead to an increase of the thruster efficiency so it has been decided in this design to leave common values of AR (around 1-2) and try higher ones.

With respect to the propellant configuration, it has been seen that according to many studies side-fed configuration increases the impulse bit when compared to breech-fed configuration. However, taking into account the goal of designing a PPT with a high value of the aspect ratio, the side-fed configuration is not as adequate as the breech-fed since the width between the two propellant bars would be small so that the spark plug was close to both of the propellant surfaces.

Once the breech-fed configuration is selected, it is possible to choose the propellant geometry: straight bar or curved one. Straight bars are easy to manufacture and easier to place into the discharge chamber. Curved bars, though, are more complicated to manufacture and need circular springs to be fed to the thruster. Since the space is limited and the design is wanted to be as simple as possible considering that curved bars would cause more problems in the positioning of the electronics around the discharge chamber so a straight bar has been chosen.

One of the main problems of loss of thruster efficiency in PPTs is the late time ablation phenomena. In order to increase the performance of our PPT, it has been decided to use a two-stage electrode configuration so that a pair of electrodes ablates the propellant bar and the other pair increases the electromagnetic acceleration.

For what concerns the electrode material, a copper-tungsten (70% W 30% Cu) alloy has been selected. This material has been chosen for its low electrical resistivity (37 $n\Omega m$) and for its good mechanical and thermal properties and reduced erosion rates, which have been proved to be particularly feasible for a PPT application [9, 41].

7.3 Electrical circuit

In this section we review the appropriate voltage booster circuits necessary to initiate an initial and main discharge in the electrode channel. The proper functionality of micro-pulsed plasma thrusters depends on the generation of an electrical arc between the two parallel electrodes. The Vacuum Arc Ignition System is responsible for creating an initial conducting path for electrons between the cathode and anode parallel plates. Field Emission is the primary mechanism for electrical breakdown in a vacuum. Field Emission is induced by an electrostatic field which causes electrons to be emitted from the cathode to the anode. There are many methods for Vacuum Arc Ignition, such as:

- High-Voltage Vacuum breakdown
- Fuse Wire Explosion
- Contact Separation
- Mechanical Triggering
- High-Voltage Surface Discharge
- Plasma Injection Triggering
- Low-voltage or triggerless vacuum arc initiation

The ideal system would function with low voltage, possess small size and weight as to fit in a 3U volume, and be would be mechanically simple as to avoid failure due to a high repetition rate of spark firings. A Triggerless Vacuum Arc Ignition system is most suitable for a micro-PPT because of its simplicity. This system needs an arc switch and a booster voltage circuit. The device used to create the initial conducting path would be a spark plug. The voltage levels to achieve ignition are within the range of 700V-2000V. Limiting factors for a Triggerless Vacuum Arc Ignition system are the spark plug size and weight, voltage booster circuit size and weight and the maximum instantaneous power available from the Cubesat to supply the voltage booster circuit.

The voltage input given by the CubeSat can be either 3.3V or 5V. The voltage booster circuit can use a device which amplifies that initial voltage. For example, there exists proportional voltage boosters that with an initial voltage of 3.3V and receiving a common current, output voltage can reach the values needed for the discharge. However, since these devices also get bigger, we could use one to get the voltage around 750V and still be small for the mission requirements.

Afterwards, we could develop a circuit involving capacitors so that the voltage received by the thruster is even higher and pulsed. With the use of switches, capacitors can be placed to be charged in parallel and then discharge in series doubling the voltage at the input.

In figure 7.2 we can see the developed circuit using normally closed switches and normally open ones. Then, in figure 7.3 we can see how the output voltage the thruster will receive will be a high voltage pulsed signal.

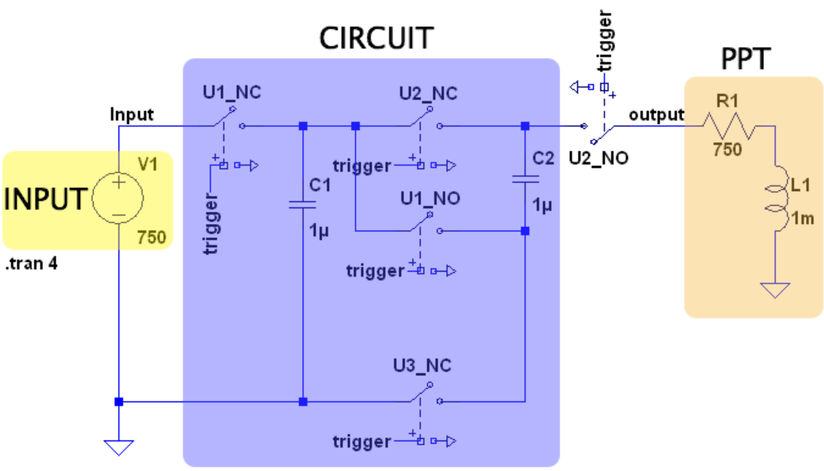

Figure 7.2: Input voltage, discharge circuit and electrical PPT schema

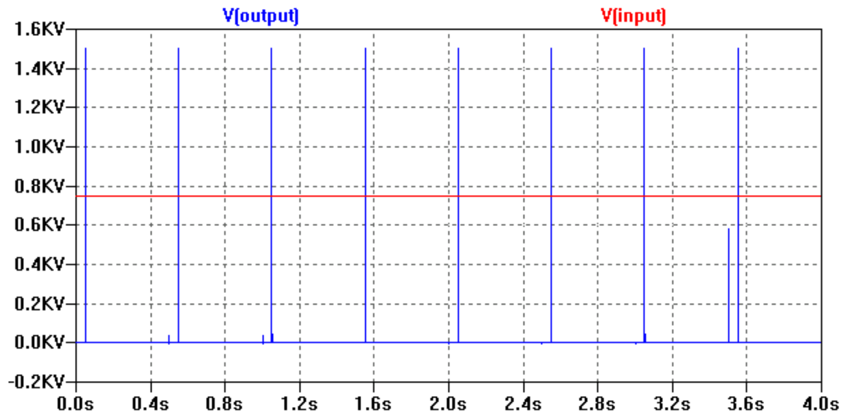

Figure 7.3: Input and output voltage values reaching the PPT

The capacitor selection is the key factor defining the maximum shot energy that could be considered for the thruster operation. This choice is one of the most critical in the entire design, and it has to be taken into account that capacitors must possess many important characteristics: they must be capable of storing a reasonably high amount of energy (few to tens of Joules) at voltages exceeding 1000 V (to assure a proper discharge initiation), withstanding high-current discharges (in the order of 10^5A) lasting only few microseconds; polarised capacitors cannot be used, because both the current and voltage waveforms are likely to reverse during the discharge; in the end, they have to survive a very large number of discharge cycles, which is determined by the particular mission, but is usually in the order of $10^6 - 10^7$.

7.4 Design

In this section it will be seen the final design of the proposed PPT. Taking into account the majority of the possible choices when designing the thruster, not all of them are possible. It is shocking that many pulsed plasma thrusters have been developed until today but they still get very poor efficiency levels.

In particular, I found interesting that the aspect ratio has such a great influence in the thruster performance. Moreover, efficiency loss is related to the Late Time Ablation effect and 2 Stage Electrode PPT's improves thruster efficiency due to fight that phenomena. Furthermore, electrode dimensions and positioning determine the PPT performance.

That is why in this PPT design it has been desired to maximise the aspect ratio but not too much because if the value of h/w is too high, important non-uniformities may arise in the electro-magnetic field, hence reducing the acceleration process efficiency [13]. Also, as we have seen many studies have confirmed that flared angle electrodes with and angle between 20 and 30 degrees improve the performance of the thruster.

Since new studies have also confirmed that tongue shaped electrodes improve thruster performance [23, 32, 34] as it has been explained in Chapter 6, it would be interesting to design a PPT with that aspect, though manufacture process gets more complex especially due to the small size of the electrodes.

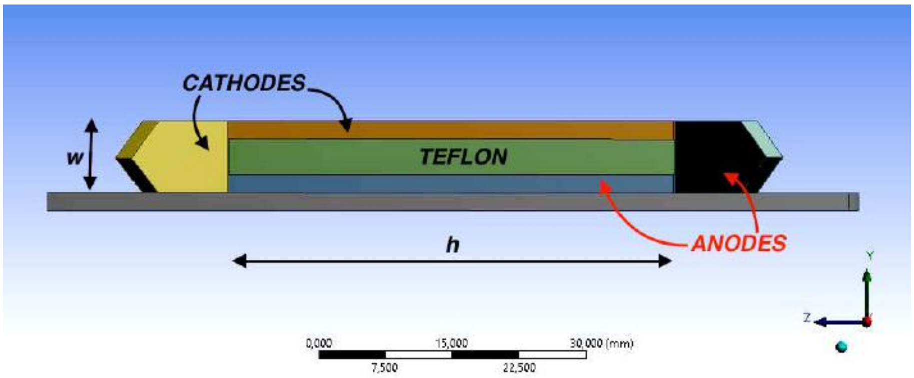

Figure 7.4: Frontal view of the proposed PPT

The first couple of electrodes between the Teflon would cause its ablation and then the other pair of electrodes would act as the main responsible for the electro-magnetic acceleration.

Both cathodes could be in contact between them and the same happens with the anodes. However, to avoid cathode/anode contact, an insulators could be used:

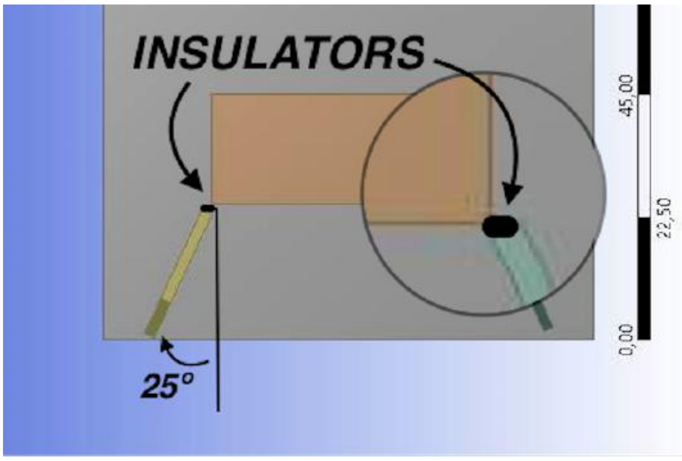

Figure 7.5: Top view of the proposed PPT using amplification

Since flare angle electrodes between 20 and 30 degrees have been proved to be the optimal, an angle of 25 degrees has been chosen in this design.

With respect to sizes, previously it was being checked the relation between the specific impulse and the E/A ratio. This design has been thought to have a energy to propellant surface ratio of $2J/cm^2$.

After that, it has to be considered the propellant area because it can not be chosen randomly but accompanied by the correspondent energy shot. For instance, if the Teflon surface was about $5cm^2$, the required shot energy would be around 10J so that the ratio keeps the desired one. Since 10J would mean having powerful capacitors that would occupy and weight too much for the saving we were trying to get, a shot energy of 2J is reasonable bearing in mind capacitors specifications. Therefore, the propellant area would be $1cm^2$.

Since it is wanted to optimise the aspect ratio we could establish a propellant bar with a surface of 5cm x 0.2cm.

It is important to check then the relation between the mass of the propellant and the specific impulse. Obviously, the less propellant available, the higher the specific impulse must be to achieve the mission requirements of total impulse. It follows the relationship:

$$I_{sp} = \frac{I_{Tot}}{\alpha_{prop} M_{prop} g_0} \tag{7.1}$$

being α_{prop} the ratio of propellant to be consumed (as a measure of security it is set in 0.9 instead of 1).

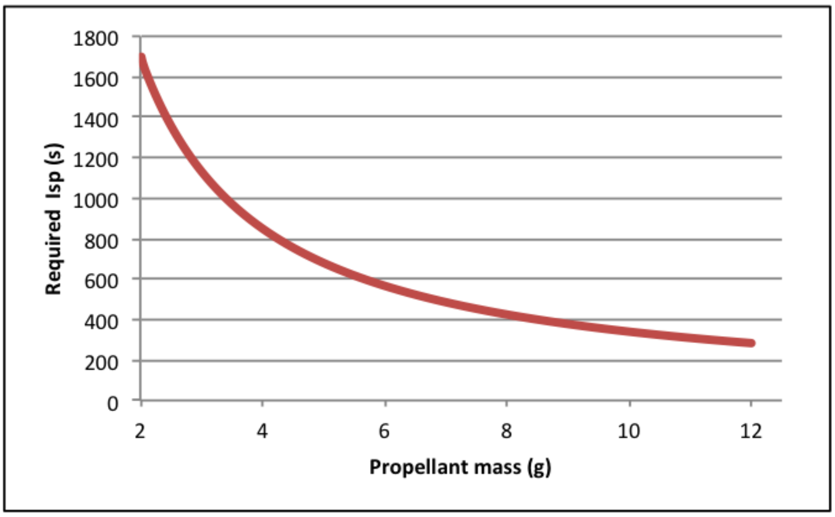

Figure 7.6: Required specific impulsed with respect to the propellant mass

Having more propellant means there is no need of it producing such a great impulse; however, since there are strict sizes and weights due to the limited space and mass restrictions, and taking into account the Guman curve (the most restrictive) to know the possible specific impulses with respect to the E/A ratio, it can be seen that it would be possible to get specific impulses higher than 400s, so a mass propellant of 8g (requiring around 400s of I_{sp} seems adequate.

Taking into account the mass and the surface measurements, we can check the third dimension:

$$M_{prop} = \rho_{teflon} A_{prop} L_{prop} \tag{7.2}$$

being $\rho_{teflon} = 2.2g/cm^3$

$$L_{prop} = 3.63cm$$

which is a possible measure taking into account the space available so the propellant bar would be 5 x 0.2 x 3.63 cm^3.

With these dimensions, taking into account the electrode common thickness of around 2mm, the Aspect Ratio h/w would get a bit higher than 8, which would be beneficial for instance to minimise the shot to shot mass bit variations. However, electrode dimensions still need to be optimised so that this pulsed plasma thruster gets the optimal results.

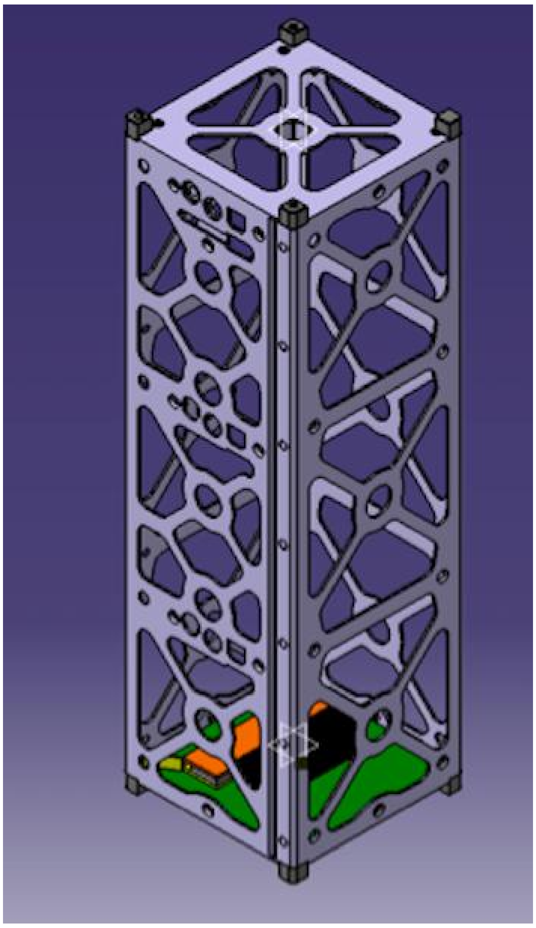

Figure 7.7: PPT inserted in a 3U CubeSat

8

Extra activities

In this chapter topics will not be related directly with the study of a pulsed plasma thruster but to explain complementary stuff I have been involved during this semester.

Zenith is an extracurricular student group I had the pleasure to meet thanks to my mentor Paulo Greco. When I first went to my mentor it was for one simple and huge thing: Space. This student group believes in the power of a high-altitude balloon as a possible way to place satellites into space. This semester it was proposed to them a biology experiment to test how bacteria would react up high. This first mission has been called Garatéa.

INPE is the Brazilian National Institute for Space Research, which is developing amazing projects through extraordinary researchers that show their passion about what they do best: science.

ITA is the prestigious Aeronautical Institute of Technology, education reaches the highest possible levels in Brazil, where clever students are graduating each year, developing other astonishing studies as in the INPE.

8.1 Zenith

Zenith's first mission was an astrobiology experiment to test some extreme bacteria and organic molecules into stratosphere in order to understand the limits of the life we know and determine if they can live in extremes environments such as Mars' and outer space's.

This project involved for the group research in many areas, from structures until internal software passing through aerodynamics, electronics, financial and more.

Each part of the group focused in one area and since my interest and knowledge is greater in aerodynamics, the development of the parachute used is explained below.

8.1.1 Parachute development

Initializing studies about a confection of a parachute, there was a crucial aspect: decide what type of parachute to use. Each type of parachute has properties and characteristics defined by its formats, size, drag coefficient and others. For these reasons we could choose the best parachute model that would minimize the falling speed and consequently the impact with the ground.

It was essential to recover the scientific load and the device with collected data (SD card) in perfect conditions to analyze the results and continue the astrobiology experiment.

The drag force acts in opposition to the weight force when a body is suffering a free fall, this force assumes an opposite direction to the motion, is given by the following expression.

$$F = kAv^2 \tag{8.1}$$

Where A is the cross-sectional area of the body and v its speed, K is the constant, which depends of the environment and the aerodynamics of the body. The phenomenon of free fall of a body at high altitudes, with the presence of a parachute, is divided into 3 basic steps:

- In the first moments, the speed of the body is still low, so you can despise the drag force during this period.

- After a moment, begins a movement accelerated, because the weight force is still greater than the drag force, resulting in a downward acceleration.

- When the drag force, by the parachute action, stay equal to the weight force, the body reaches its terminal velocity, smaller e safer for the impact with the ground. The terminal velocity can be calculated by the following expression:

$$v^2 = \frac{mg}{kA} \tag{8.2}$$

The most important factor to study, in order to optimize the action of parachute, is the drag coefficient (Cd) of the object/body in the surroundings. It is through it that we have a better understanding of your performance. The coefficient can be calculated using the equation below:

$$C_d = \frac{2F_d}{\rho v^2 A} \tag{8.3}$$

Note that it is dependent on the speed, the drag force, the air density and the area of the moving object, so the geometry of the body is very important for the choice of the best type of parachute.

8.1.1.1 Choice of type of parachute

There are many predefined types of parachutes, each with a particular type of application recommended. For the launch of the probe in question, which takes a payload of about 4 lb, it was necessary to choose and adapt a parachute that manage certain characteristics, such as terminal velocity, weight, cost, number of shroud lines, etc. The following table shows, for example, for various types of parachutes, a range of variation for the C_d.

Type of parachute	Typical Cd range
Flat Circular	0.75-0.80
Hemispherical	0.62-0.77
X-Form	0.60-0.85
Conical	0.75-0.90
Bi-Conical	0.75-0.92
Tri-poly conical	0.80-0.96

Table 8.1: Drag Coefficients depending on the type of parachute

It is seen that the bi-conical type and tri-poly conical are parachutes with high drag coefficients, making them very efficient in several applications. These types of parachutes are better for the transportation of heavy loads, because they give more stability in flight. But as the launch of the probe, under study, is a relatively light experiment, is likely to become a turbulent descent and by the high number of canopy shroud lines these types of parachute they have great chances of getting curled, stopping the full opening of the parachute.

Thus, analyzing tables, comparing the different models, considering the number of strings, we could say that the cross-type are simple construction parachutes, have a good drag coefficient and are able to supporting the sued weight.

8.1.1.2 Sizing, calculations and parameters

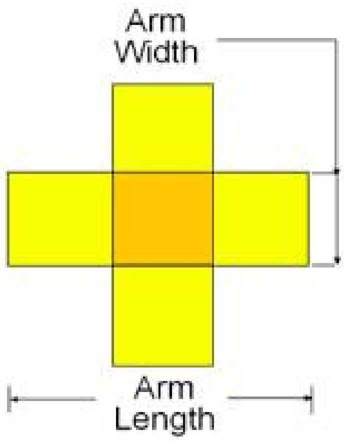

Figure 8.1: Schema of a Cross-Type Parachute

The image above represents schematically a model of a parachute of type "X"(cross-type), it is possible to observe two basic dimensions, which are bases for the calculation of the area of the parachute, their rate of descent and other factors.

For the calculation of the area the following formula is used: W_a is the parachute arm width and D_c the parachute diameter, in this case, the arm length. It is important to note that the proportion between the measures of arm length and width should be followed; it is recommended that the length has to be 3 times greater than the width.

Using a equation to calculate the descend rate of the system, it was possible to scale the parachute, some spreadsheet and online information were used to get more accurate results.

$$V_t = \sqrt{\frac{2W}{C_d S_0 \delta}} \tag{8.4}$$

So a prototype was made and tested by the group throwing it with a test load. When good results were obtained another parachute was constructed. Besides, we used a worn paraglider to obtain a especial fabric, in this case a ripstop-nylon fabric. For these dimensions: $W_a : 6ft(0,6096m)$ $D_c : 2ft(1,8288m)$ $S_0 : 20ft(1,85806m)$

Assuming a drag coefficient of 0.85, a standard air density at sea level, for 7lb (3,18kg) payload, we get: Vt= 18,57 ft/s (5,66 m/s)

Redoing the calculations for a smaller coefficient (0.65), but with the same payload:

$V_t = 21,24ft/s(6,47m/s)$

Thus, it is clear that for a standard load of 3 kg, a 6 feet diameter parachute reaches a final speed of 5.66 m/s and 6.47 m/s, depending on its drag coefficient. Taking into consideration the delicacy of the experiment, we decide to use a 1 metre cross parachute (according to Richard Nakkas Experimental Rocketry Web Site) which has a 1,5 meter diameter, approximately.

8.1.2 Results

After analyzing the entire flight video, that the chosen model worked well, the probe did a very stable journey and in the impact with the ground did not spoil any part of the structure so it can be used in futures projects.

This first mission was a success but the team is already getting ready for the next one because Garatéa was only the first of many to come.

Figure 8.2: Photo taken at the Garatéa gondola in the stratosphere, with bacteria being exposed (All Credits to Zenith)

8.2 INPE e ITA

8.2.1 INPE, São José dos Campos

The students at Zenith had the pleasure to visit the installations of the INPE based in São José dos Campos. Once there, we first went to the LabSim and were shown the engineering models of the CubeSats they are developing there: NanosatC-Br1 e NanosatC-Br2.

A member of Zenith is currently doing a internship at that department and really made us see researchers love what they do.

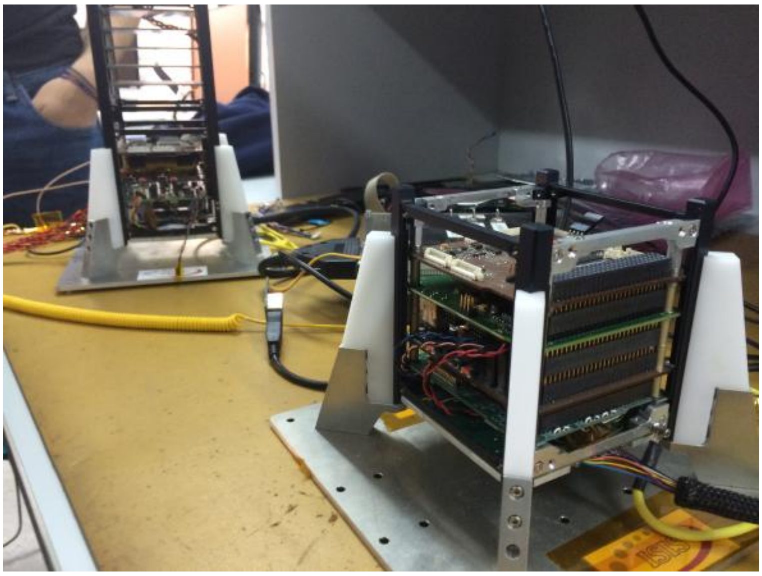

Figure 8.3: Engineering models of a NanosatC-Br1 and NanosatC-Br2

Afterwards, we visited he LIT (Integration and Tests Laboratory) by the hand of José Sérgio de Almeida and got astonished about the first-level equipment they have. A 6m x 8m space simulation chamber gets the main attention, along with the various thermal vacuum chambers, a environmental test chamber, a thermal shock chamber, a Walk-in thermal chamber, an anechoic chamber, shakers for vibrational tests and more.

Figure 8.4: Zenith student group at LIT laboratory of INPE

It is interesting that these installations have tested satellites and space equipment from Argentina's until USA's.

8.2.2 ITA

After that visit we went to ITA and met the professional team developing the ITASAT-1, a satellite that is part of the AEB (Brazilian Space Agency) plan of increasing the interest in space exploration. This satellite is a 6U CubeSat, bigger than the ones developed at INPE. ITASAT-1 counts with many sensors, GPS and even a camera, among other equipment.

Figure 8.5: Perspective projection of the modules distribution in the 6U structure (Credits: ITA)

8.2.3 LCP, INPE, Cachoeira Paulista

From the day I started researching about pulsed plasma thrusters, I noticed Rodrigo Intini Marques was an expert in the field. After the projects he developed at University of Southampton about PPTs, he came back to Brazil to work in the Associated Laboratory of Combustion and Propulsion of INPE. Until now, much progress has been made thanks to that laboratory where there are high-vacuum chambers to test these thrusters and even bigger chambers to test chemical propulsion systems.

Not only a good researcher but also an extremely kind person, Rodrigo invited my mentor, a doctorate student and me to visit this amazing laboratory of the Brazilian National Institute for Space Research.

We were shown much of the equipment that is available there and offered us the possibility of testing a PPT if we are going to develop one.

Moreover, we all discussed about this kind of thrusters that might be essential for the near future when capacitors are much powerful with smaller sizes. We were shown two very interesting PPTs developed and tested there [8, 18].

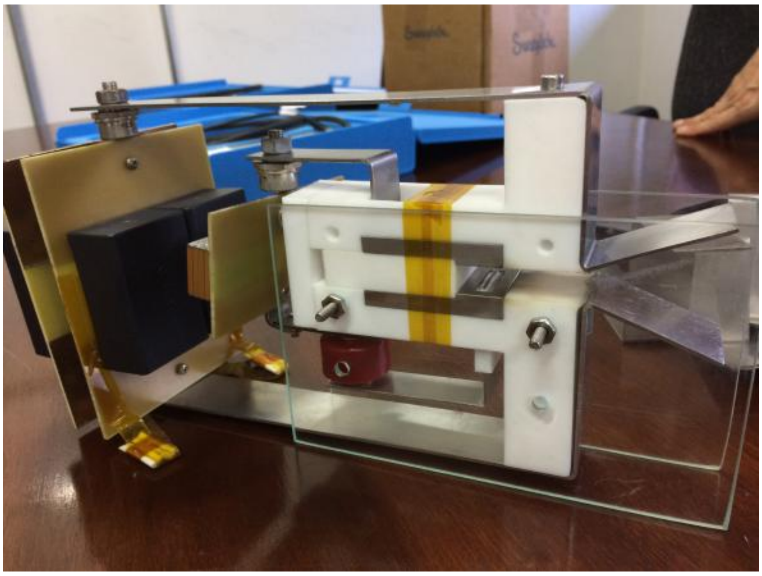

Figure 8.6: Pulsed Plasma Thruster developed at INPE [8]

9

Conclusion and Future Work

The main goals of this project was to study pulsed plasma thrusters, find ways to optimise them and propose a new design. PPT's efficiency is still low and there is a wide improvement range so more research is yet to come.

Initially, our intention was to simulate a PPT with a software, such as Comsol (because it can handle at the same time electric circuits, magnetic fields and plasma), but after trying to we discovered it was not possible yet due to the low pressure (vacuum, space conditions) and the perpendicular magnetic field. In fact, it is a specific limitation of the plasma module, which cannot currently model magnetrons and space thrusters due to the fact that the perpendicular versus cross field electron mobility and diffusivity can be on the order of 10^8, which poses severe numerical challenges and inevitably there is unphysical numerical diffusion across the magnetic field lines. Nevertheless, in the near future computation will be more advanced and probably pulsed plasma thruster will be modelled easily.

As for now, it has been extremely interesting to check many possible ways to optimise PPTs through all the studies that have been already performed. In particular, both the Aspect Ratio of the discharge chamber and the E/A ratio since they have a strong influence in the efficiency and the specific impulse produced by the thruster, they are crucial to improve to meet the mission requirements.

9. CONCLUSION AND FUTURE WORK

In this report it has been proposed an initial PPT design bearing in mind the possible ways to increase efficiency of it. However, there are still many analysis to perform so that this thruster is reliable and in the end taking part of an actual CubeSat.

As future work recommendations, it would be perfect to develop a model to evaluate and optimise all the thruster's parameters. In fact, a trustful and complete model is almost necessary so that there is no need of making different PPTs experimentally due to the infinite number of conditions and parameters that can change.

To conclude, I just hope this work can be helpful for Ash in his doctorate, which I trust it will make advancements in the pulsed plasma thruster improvements; and little by litte, great things can be achieved.

References

[1] Scharlemann C. A. Investigations of thrust mechanisms in a water fed pulsed plasma thruster. *Dissertation, Department of Aeronautical and Astronautical Engineering, The Ohio State University*, 2003. 17, 39

[2] G.; Orlov M.; Popov G.A. Tyutin V.; Yakovlev V. Posokhin V. Razumov P. Alexeev Yu. Kazeev M.N. Antropov, N.N.; Diakonov and F. Darnon. High efficiency ablative pulsed plasma thruster characteristics. *3rd International Conference on Spacecraft Propulsion, Cannes, October 10-13*, 2000. 23

[3] R.L. Burton and P.J. Turchi. Pulsed plasma thruster. *Journal of Propulsion and Power*, vol. 14, No. 5:716–735, September-October, 1998. 8, 21, 22, 24, 44

[4] Rysanek F. Antonsen E.L. Wilson M.J. Burton, R.L. and S. Bushman. Pulsed plasma thruster performance for microspacecraft propulsion. *Micropropulsion for Small Spacecraft. M. M. Micci and A. D. Ketsdever*, Eds.: AIAA, 2000, Progress in Astronautics and Aeronautics Series. 8

[5] Wilson M.J. Burton, R.L. and S. Bushman. Energy balance and efficiency of the pulsed plasma thruster. *34th AIAA/ASME/SAE/ASEE Joint Propulsion Conference and Exhibit, Cleveland, OH, USA, July 13-15*, 1998. 8

[6] Marques R. Intini Coletti, M. and S.B. Gabriel. Design of a two-stage ppt for cubesat application. *The 31st International Electric Propulsion Conference, University of Michigan, Ann Arbor, Michigan, USA, Semptember 20-24*, 2009. 23

[7] Laperriere D. D. Electromechanical modelling and open-loop control of parallel-plate pulsed plasma microthrusters with applied magnetic fields. *Masters Thesis, Department of Mechanical Engineering, Worcester Polytechnic Institute, 100 Institute Road, Worcester, MA 01609-2280*, 2005. 27, 33, 35

[8] Paula Fin. Influência da geometria dos eletrodos secundários no desempenho de um propulsor de plasma pulsado de dois estágios. *São José dos Campos, INPE*, 2014. iv, 64

[9] Waelbroeck F. L Fitzpatrick R., Hazeltine R. D. Introduction to plasma physics: A graduate course. *University of Texas at Austin*, 2006. 31, 46

[10] P. Gessini and G. Paccani. Ablative pulsed plasma thruster system optimization for microsatellites. *27th International Electric Propulsion Conference, Pasadena, CA, USA, October 15-19*, 2001. 22, 44

[11] FRANCESCO GUARDUCCI. Design and testing of a micro ppt for cubesat applications. 2012. iv, 45

[12] L.B. Holcomb. Satellite auxiliary-propulsion selection techniques. *JPL, Pasadena, CA, USA*, 1971. 8

[13] R. Jahn. Physics of electric propulsion. *McGraw-Hill, New York*, 1968. iii, 8, 15, 16, 17, 50

[14] S. Kuroki K. Miyagi. Influence of electrode configuration of a liquid propellant ppt on its performance. *Joint Conference of 30th ISTS, 34th IEPC and 6th NSAT, Kobe-Hyogo, Japan, July 4 10*, 2015. 22, 25

[15] Pencil E. J. Haag T. Kamhawi H., Arrington L. Performance evaluation of a high energystpulsed plasma thruster. *AIAA 2005-3695, 41 Joint Propulsion Conference, Tucson, Arizona*, 2005. iii, 11, 18

[16] Inoue S. Kimurra I., Yanagi R. Preliminary experiments on pulsed plasma thrusters with applied magnetic fields. *13th International Electric Propulsion Conference, San Diego, California*, 1978. 35

[17] Herdrich G. Fasoulas S. Roser H.P. Koch M. Lau, M. and T. Hintze. impd system study and high voltage power supply subsystem development at irs. *32nd International Electric Propulsion Conference, Wiesbaden, September*, 11-15, 2011. 24, 25, 41

[18] Luis Francisco Chrispim Marin. Anlise do desempenho de um propulsor a plasma pulsado de dupla descarga atravs da variao da distribuio de energia entre os seus dois estgios. *So Jos dos Campos : INPE*, 2014. 64

[19] Gabriel S.B. Marques, R. Intini and F. de S. Costa. High frequency burst pulsed plasma thruster research at the university of southampton. *30th International Electric Propulsion Conference, Florence, Italy, September 17-20*, 2007. 23

[20] R. Intini Marques. A mechanism to accelerate the late time ablation for the pulsed plasma thruster. *PhD, Astronautic Reaseacrh Group, School of Engineering Sciences, University of Southampton, Southampton, UK*, 2009. 23

[21] I.G. Mikellides and P.J. Turchi. Optimization of pulsed plasma thrusters in rectangular and coaxial geometries. *26th International Electric Propulsion Conference, Kitakyushu, Japan, October 17-21*, 1999. 23

[22] J. Mueller. Thruster options for microspacecraft: A review and evaluation of state-of-the-art and emerging technologies. *Micropropulsion for Small Spacecraft, Progress in Astronautics and Aeronautics*, 187edited by Micci, M. and Ketsdever, A., AIAA , Reston, VA, 2000. 44

[23] Albertoni R. Nawaz, A. and M. AuweterNKurtz. Thrust efficiency optimization of the pulsed plasma thruster simpnlex. *Acta Astronautica*, 67:440–448, 2010. 18, 41, 50

[24] Fukagawa H. Kera S. Yoshimura D. Morikawa E. Deki K. Ueno N. Ono M., Yamane H. Possibility of the fermi level control by vuv- induced doping of an organic thin film: Polytetrafluoroethylene. *Proc. Int. Symp. Super- Functionality Organic Devices, IPAP Conf. Series 6*, pages 27–30. 31

[25] Kamhawi H. Arrington L.A. Pencil, E.J. and W.B. Warren. Evaluation of alternate propellants for pulsed plasma thrusters. *27th International Electric Propulsion Conference, Pasadena, CA, USA, October 15-19*, 2001. 24

[26] Waltz P.M. Analysis of a pulsed electromagnetic plasma thruster. *Masters Thesis, Massachusetts Institute of Technology, Department of Electrical Engineering, Cambridge, MA*, 1969. iii, 32, 33

[27] G.A. Popov and N.N. Antropov. Ablative ppt. new quality, new perspectives. *Acta Astronautica*, 59:175–180, 2006. 23

[28] V. J. Lappas P.V. Shaw. Mathematical modeling of a high efficiency pulsed plasma thruster for microsatellites. *57th International Astronautical Congress, International Astronautical Congress (IAF)*, Valencia, Spain, 2006. iii, iv, v, 27, 32, 33, 34, 39, 40

[29] Z. He F. Zhang J. J. Wu R. Zhang, D. X. Zhang. Influence of electrode flare angle on the performance of pulsed plasma thruster. *Applied Mechanics and Materials*, 232:353–358, 2012. iii, 35, 36, 37, 38

[30] Campbell M Rayburn C. Development of a micro pulsed plasma thruster for the dawgstar nanosatellite. *AIAA 2000-3256, 36th Joint Propulsion Conference, Huntsville, Alabama*, 2000. 16

[31] Mattick A.T Rayburn C., Campbell M. Pulsed plasma thruster system for microsatellites. *Journal of Spacecraft*, 42, No.1, 2005. iii, 17, 18

[32] Komurasaki K. Schonherr, T. and G. Herdrich. Study on plasma creation and propagation in a pulsed magnetoplasmadynamic thruster. *Word Academy of Science, Engineering and Technology*, 74:563–569, 2011. 18, 41, 50

[33] Komurasaki K. Kawashima R. Arakawa Y. Schonherr, T. and G. Herdrich. Evaluation of discharge behavior of the pulsed plasma thruster simpnlex. *46th AIAA/ASME/SAE/ASEE Joint Propulsion Conference and Exhibit, Nashville, TN, USA, July*, pages 25–28, 2010. 41

[34] Komurasaki K. Nees F. Koizumi H. Arakawa Y. Manna S. Lau M. Herdrich G. Schonherr, T. and S. Fasoulas. Mass and plasma characteristics in the current sheet of a pulsed plasma thruster. *32nd International Electric Propulsion Conference, Wiesbaden, September*, pages 11–15, 2011. 41, 50

[35] P. Shaw and V. Lappas. Modeling of a pulsed plasma thruster; simple design, complex matter. *Space Propulsion Conference, San Sebastian, Spain, May*, pages 3–6, 2010. 21, 41

[36] A. Solbes and R.J. Vondra. Performance study of a solid fuel-pulsed electric microthruster. *Journal of Spacecraft*, 10, 6, January:406–410, 1973. 8

[37] Vondra R. J Solbes A. Performance study of a solid fuel-pulsed electric microthruster. *Journal of Spacecraft*, 10, No.6:406–41. 30

[38] W. M. Stacey. Fusion plasma analysis. *1st Edition, Krieger, ISBN 0894646028*, 1981. 22, 31

[39] Kurzyna J. Szelecka A. Liquid micro pulsed plasma thruster. Warsaw, Poland, 2015. 25

[40] R.J. Vondra and K. Thomassen. Performance improvements in solid fuel microthrusters. *Journal of Spacecraft and Rockets*, 9, No. 10:738–742, 1972. iii, 14, 45

[41] Choueiri E.Y. Ziemer, J.K. and D. Birx. Is the gas-fed ppt an electromagnetic accelerator? an investigation using measured performance. *35th AIAA/ASME/SAE/ASEE Joint Propulsion Conference and Exhibition, Los Angeles, CA, USA, June 20-23*, 1999. 8, 25, 46

[42] J. Ziemer. Performance scaling of gas-fed pulsed plasma thrusters. *Ph.D.Thesis, Department of Mechanical and Aerospace Engineering, Princeton University, Princeton, NJ, USA*, 2001. iii, 8, 14, 15

[43] J. Ziemer and R.A. Petr. Performance of gas fed pulsed plasma thrusters using water vapor propellant. *38th AIAA/ASME/SAE/ASEE Joint Propulsion Conference and Exhibit, Indianapolis, IN, USA, July 7-10*, 2002. 25

Declaration

I herewith declare that I have produced this paper without the prohibited assistance of third parties and without making use of aids other than those specified; notions taken over directly or indirectly from other sources have been identified as such. This paper has not previously been presented in identical or similar form to any other Brazilian or foreign examination board.

The thesis work was conducted from February to June 2016 under the supervision of Pr. Dr. Paulo Celso Greco Júnior at University of São Paulo.

São Carlos,

Xavier Almenar Cerdán